AD-A062 574 DREXEL UNIV PHILADELPHIA PA DEPT OF MECHANICAL ENGIN--ETC F/G 20/1
AN ULTRASONIC NONDESTRUCTIVE TEST PROCEDURE FOR THE EARLY DETEC--ETC(U)
AUG 78 J M CARSON, J L ROSE N00014-77-C-0607
UNCLASSIFIED NL

| OF |
AD
A062574

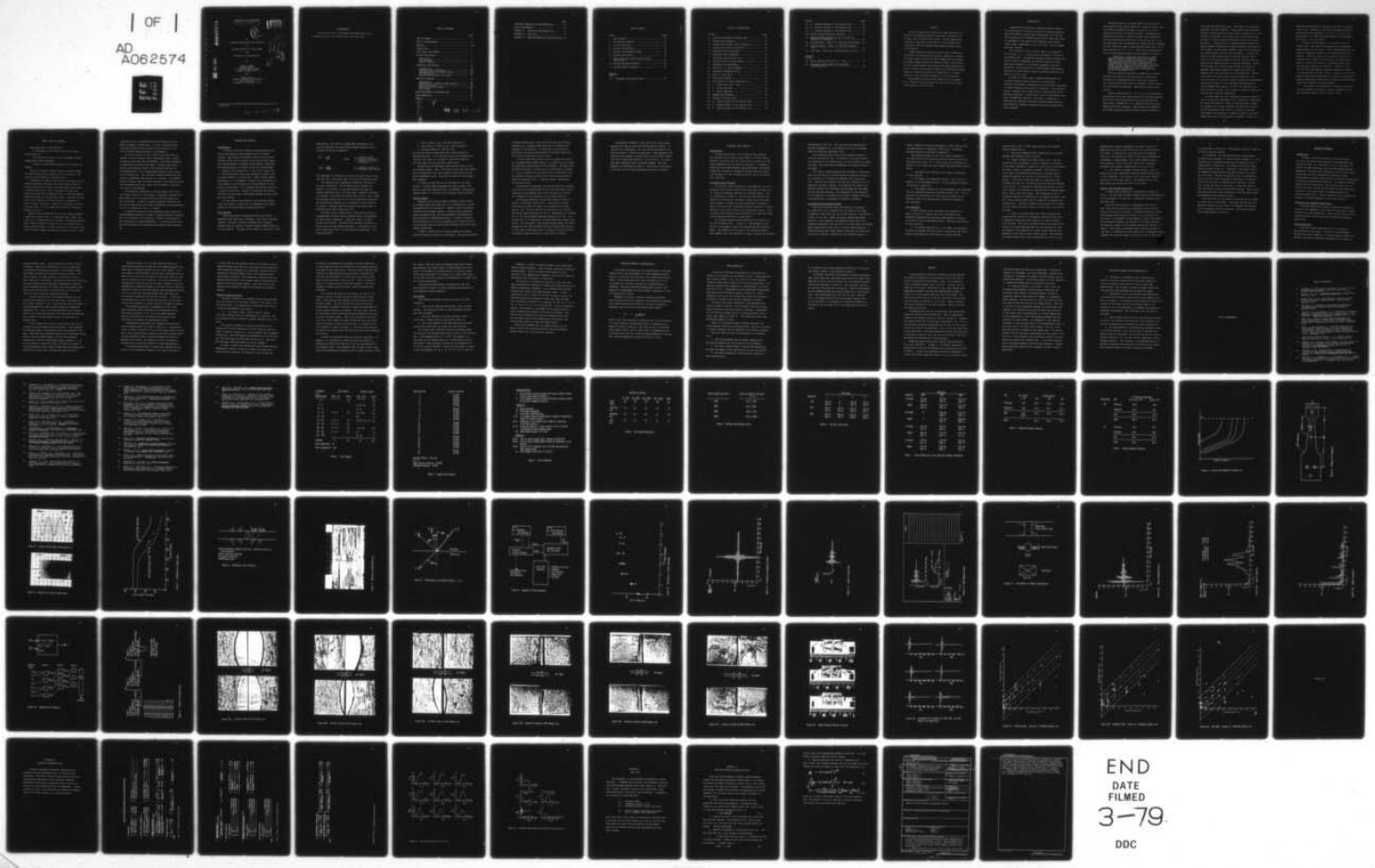

END
DATE
FILMED
3-79
DDC

An Ultrasonic Nondestructive Test Procedure for The Early Detection of Fatigue Damage and The Prediction of Remaining Life

by

James M. Carson+
Research Engineer
E. I. Dupont-De Nemours Company
Seaford, Delaware 19973

and

Joseph L. Rose
Professor of Mechanical Engineering
Drexel University
Philadelphia, Pennsylvania 19104

+ Graduate Student in Mechanical Engineering and Mechanics from July 1976 to June 1978

ACKNOWLEDGMENTS

The authors would like to acknowledge Kruatkramer-Branson, Incorporated for the use of the computer system used in this study.

TABLE OF CONTENTS

LIST OF TABLES

LIST OF ILLUSTRATIONS

ABSTRACT

The goal of nondestructive testing may be simply expressed as the detection and complete specification (size, shape, orientation, etc.) of flaws. This is seldom possible, however. The most dangerous flaw is one that is crack-like or that serves as a crack initiation site. A procedure to detect and estimate fatigue damage occurring at such a site is reported.

A computer based data acquisition system is used to analyze data from 2024-T4 Al fatigue specimens containing a through hole. Specimens are fatigue loaded to produce a spectrum of damage levels and interrogated using a simple contact 10 MHz shear wave system. Features selected from the signal amplitude time, spectrum, and cepstrum signatures are used in a computer learning network to make an early detection of fatigue damage and a quantitative prediction of remaining life. A scanning microscope is used to examine the damage at the limit of detection.

Fatigue damage was sensed with 92% success after 10% of specimen life. Estimates of damage were made within $\pm$ 20 of the actual fatigue life percentage for 76% of the data.

INTRODUCTION

Nondestructive inspection techniques seek to improve the reliability of various structures by detecting material flaws and defects either during manufacture or in service. The ultimate goal of nondestructive testing (NDT) may simply be expressed as the location and complete specification (size, shape, orientation, etc.) of a flaw. This is seldom possible, however.

Even assuming a flaw is found, NDT can not determine how critical it is. It may thus be necessary to discard a serviceable part. Engineering experience might indicate that certain types of responses from certain materials, manufacturing processes, or structures represent a critical situation. The disciplines of stress analysis and fracture mechanics can help locate critical structural areas and help define a critical flaw.

In order to attack today's complex NDT problems, an organized approach making the best use of available inspection procedures, instrumentation and advanced techniques in signal gathering and analysis is required. These elements must be combined with as much physical understanding of the problem as possible. Inattention to any of these details can ruin a prospective solution. This work, in addition to attacking the important problem of fatigue damage detection and estimation, suggests procedures that can be extended to other problems.

One definition of a critical flaw is a flaw which is crack-like or which easily serves as a crack initiation site. It has been estimated that some 75 to 95% [1, 2] of all mechanical failures are fatigue related. Considering the catastrophic nature of failure by rapid crack propagation and the foreshortened lifetime of a fatigue failure, it is not surprising that the detection of cracks and the estimation of their length has been a recurring and recent topic in the NDT literature [3, 4, 5, 6, 7]. Even with this background the Air Force Systems Command Design Handbook [8] states:

> Examination of pre-existing cracks in aerospace structures exposed by analysis, following complete failure of the parts involved, indicates that conventional production quality control nondestructive testing cannot confidently be expected to find surface cracks less than 0.150 inch in the greatest dimension. This limit can be substantially reduced by special techniques and skills at increased costs.

The work reported here seeks to improve the reliable detection of cracks and fatigue damage by using a well conceived but straightforward and realistic ultrasonic test system coupled with recently developed signal acquisition and analysis procedures. Background in these areas follows.

Several investigators [9, 10, 11, 12] have designated ultrasonics as the test method having the greatest potential for solving flaw detection and classification problems. Specifically, Packman et al [9] examined the use of x-ray, magnetic-particle, penetrant, eddy-current and ultrasonic techniques to detect surface fatigue cracks initiated at

micro-weld solidification spots. The shear wave ultrasonic technique was found superior. Often studies are performed to measure a crack dimension such as length or depth [6, 13, 14]. As might be expected, the probability of detection and the accuracy of length estimation decrease as the crack length decreases. A Boeing study [14] demonstrated an inspection system capable of detecting aircraft fastener hole cracks of .030 inches in radial depth; however, there was no detection for smaller flaws, and poor size estimation. It was noted that while eddy current methods could be used for small cracks, the ultrasonic method was chosen to avoid the cost and possible damage involved in removing fasteners. Shankar and Mucciardi [15] recently demonstrated the ability of computer aided signal analysis to extend the limits of fastener hole crack detection and size estimation. Rather than measure the crack length Green and Pond [16], and Joshi and Green [17] used ultrasonic attenuation measurements through the volume of a test specimen and detected bulk fatigue damage after some 70 to 90% of the specimen life. This was prior to being able to detect a specific crack with conventional ultrasonic techniques.

For many years the main ultrasonic detection characteristic has been the amplitude of the reflected or transmitted RF signal displayed in a video or rectified mode. Simply, the presence of a signal indicates the presence of a flaw and the amplitude of the signal is related to its size. Krautkramer [18] developed a system to quantify such amplitudes based upon a flat bottom hole standard. However, an

amplitude based system is ambiguous when used to classify a real flaw. Problems in this area have been pointed out and alternatives suggested [3, 19, 20, 21, 22, 23, 24]. Nevertheless, the amplitude based system is the procedure most used in the field today.

A number of investigators, following the lead of Gericke [20], have used the information in the spectral representation of the signal. Other transformations of the signal to emphasize certain of its characteristics are possible. Recently, Rose [25] has shown the ability to differentiate a variety of artificial flaw types such as sharp vs. smooth and single vs. multiple through holes using pattern recognition algorithms. Mucciardi et al [15, 26] have used adaptive learning networks to measure flat bottom holes and crack lengths. Raisch [27] has shown pattern recognition procedures to be useful in measuring a material performance characteristic (adhesive bond strength) rather than finding a particular defect.

It is against this background of locating cracks and of using advanced techniques to extract information from the ultrasonic signal that this study is set.

STUDY GOALS AND SUMMARY

The objectives of this study are:

. to distinguish a flaw from a flaw with a crack growing from it.

. to determine how early in its development fatigue damage/cracks can be detected.

. to make a quantitative prediction of the extent of damage.

Details of specific test procedures, specimen design, and signal analysis are contained in later sections. An overview of the problem is presented here.

A knowledge of loading conditions, stress analysis, and fracture mechanics indicates that cracks tend to form at certain sites and in certain structural areas, and to grow in certain directions. This is particularly true when artificial sites such as fastener holes, cooling passageways, threaded sections, or keyways are present. This may be less true if the formation sites are natural in form, such as voids or metal inclusions. However, the artificial sources have been shown to be the predominant sources of cracking problems [28, 29].

Most of the investigators to date have tried to detect a crack of a certain size. In some cases this "crack" was a saw cut or a machined slot, in others a fatigue crack grown from a starter scratch or notch, and in a few cases actual cracks have been used. The work presented in this paper uses a plate fatigue specimen containing a through hole as a crack

initiation site. No modification of the through hole was made to produce a single crack. In fact, a multiple crack was always formed in the vicinity of the hole due to the cyclic reverse bending applied to the specimen.

At various points in their fatigue life, the test was stopped, and the specimens were interrogated using a simple ultrasonic shear wave test arrangement. The entire inspection was made from one side of the plate. Fixtures were used to locate the transducer normal to the expected direction of crack propagation at two predetermined locations with respect to the through hole. The ultrasonic waveforms were digitized, stored, transformed, and analyzed on a computer. An adaptive learning network (ALN) was used to develop a correlation between the characteristics of the signal and the percent of fatigue life seen by the specimen.

This produced a detection of fatigue damage after 10% of the fatigue life with a 92% success. Estimates of damage were made within $\pm$ 20 of the actual fatigue life percentage for 76% of the data. A study of fracture surfaces indicates that the single crack size at the limit of detection was approximately .020 in. in length and .030 in. in depth.

It should be noted that this procedure avoids progressing from measuring crack size, through a fracture mechanics analysis, and to a calculation of criticality. Rather it goes directly to a prediction of system performance. It should also be noted that the ultrasonic test procedure was realistic for inservice use.

FATIGUE TEST DETAILS

Introduction

A variety of factors influence fatigue behavior and create the typically large scatter found in fatigue testing. Among them are residual stress, stress raisers, surface finish, and variations in the fatigue test itself due to misalignment or changes in the loading conditions. The fatigue process is usually broken into three stages: 1. formation of a microcrack, 2. slow crack growth, and 3. final rapid crack growth and catastrophic failure when the crack reaches a critical size. Under a given loading environment it is reasonable to expect that the scatter is more related to the formation of the microcrack than the rate of crack growth. It is assumed that failure occurs at a constant crack size. Figure 1 illustrates this scatter and shows the non-linear relationship between fatigue cycles and crack length.

To help control the scatter in this testing program steps were taken to insure that all specimens were nearly identical and tested under the same conditions.

Test Specimen

Cracks were grown in standard Krouse type fatigue specimens made from 2024-T4 aluminum. This type of specimen (Figure 2) employs a constant thickness and a linearly tapered width to achieve a constant maximum bending stress in its test section. The apex of this taper is the point of load

application. The load (P), stress (σ) and deflection (Y) can be related for this cantilever mounted specimen using a strength of materials approach.

$$\sigma = \frac{PL^2}{bh^2}$$

where b = specimen width
h = specimen thickness
L = length from apex to width at b.

$$Y_{max} = \frac{6L^3P}{bh^3E}$$

$\frac{b}{L}$ = constant (.2000) in specimen test section

This approach is reasonable as long as the apex angle is less than 40° [30]. This angle was 10.42° for the specimens used.

The specimens were prepared by Laboratory Devices Co., San Jose, California. The alignment holes, labeled A in Figure 2, and the hole in the test section were made at Drexel University using a drilling guide. Specimen thickness is a nominal .251 inches and varies from .2505 to .2515 inches. The specimen surface was left in the as fabricated condition. The longitudinal specimen axis is parallel to the direction of rolling. Specimen edges were broken with emery paper in accordance with ASTM suggestions [31].

The test section through holes, which serve as stress concentrators and thus crack initiation sites, were prepared to insure their uniformity. Steps were taken to insure minimal cold working. The hole making process consisted of two drilling and one reaming operation. A specimen jig and drill guides were used in the two drilling operations. The process follows:

1. drill .0785 in. dia. hole (#47 wire drill)
2. drill hole to .0890 in. dia. (#43 wire drill)
3. chucking reamer to .0995 in. dia.

Drilling and reaming operations used a water soluble oil lubricant/coolant. A two step hole gage having diameters of .0995 in. and .0988 in. was made to check hole diameters. All holes were found to be within these limits.

The drilling jig mentioned above was also used to drill the alignment holes. Note from Figure 2 that the test section hole is equidistant from the alignment holes and two of the driver attachment holes. This fact is used in the ultrasonic test sequence.

In order to avoid testing the specimens in the order drilled, a random number procedure was used to select the order in which the specimens were to be tested. The specimen labeled number 1 is thus the first randomly chosen specimen.

Fatigue Loading

Specimens were cyclic loaded to produce various levels of fatigue damage and cracks and not to determine the fatigue characteristics of the material. However, since the desired correlation was between number of cycles and the ultrasonic signal characteristics, the fatigue machine characteristics were monitored, as demonstrated below, to insure a constant loading condition for all the specimens and to avoid variance in the fatigue life or crack growth characteristics due to the loading conditions.

A Budd Co. Model VSP-150 variable speed plate bending machine was used to fatigue the specimens. This machine applies

a constant deflection to one end of the cantilever mounted specimen via a variable throw crank and a connecting rod attached to the specimen. A horizontally and vertically adjustable vise allows adjustments for specimen length and for various desired mean stress levels.

A strain gaged specimen was used to adjust the loading to a reverse bending (mean stress = 0) condition and to check the operating characteristics of the machine. The test speed was 2000 cycles/min. (30 ms/cycle) as illustrated in Figure 3. Figure 4 shows that this machine did not produce a start up overshoot although several ($\sim$ 20) cycles are required to reach the operating rate. A machine counter counts every one hundred cycles.

The machine's adjustable vise was modified with a pinned steel block that was designed to mate with the holes in the clamp end of the specimen and insure the accurate location and alignment of each specimen in the fatigue machine.

Preliminary specimens were fatigue loaded in order to choose a convenient loading level. The results of these four tests are shown in Figure 5 and compare with similar data in Ref. [32] for 2024-T4 Al also shown in the figure. The chosen test deflection of .405 in. corresponds to a loading of 71.1 lb. and a nominal specimen stress of 34.0 Ksi. The through hole in the specimen of course produces a larger local stress. The low cycle - high stress fatigue region was chosen because of test time considerations and because small errors in the stress (deflection) due to loading in this region will not produce large variations in the cycles to failure.

Periodically through the test series the strain gaged specimen was used to check the fatigue machine loading. No variation was discovered. The test series consisted of the fatigue testing of twenty-two specimens. Some specimens were ultrasonically tested at several points during their fatigue life while others were tested at only one point. All specimens were inspected prior to fatigue loading. The test program is illustrated in Table 1. Statistics on the cycles to failure for the various specimens are shown in Table 2.

ULTRASONIC TEST DETAILS

Introduction

As mentioned earlier, the ultrasonic test employed was designed to be realistic and simple, to tend to remove operator influences from the testing and to perform the complete inspection from one side of the plate. It should be noted that even sophisticated signal processing and pattern recognition schemes are doomed to failure unless the basic test equipment is well understood and the testing procedure well conceived.

Ultrasonic Test Procedure

An ultrasonic test consisted of interrogating the hole/potential crack region from two locations with a 10 MHz, 1/4 in. diameter transducer mounted on a plexiglas wedge. This is illustrated in Figure 6. The position far from the hole (position 1) bounced the ultrasonic energy from the bottom plate surface to inspect the top surface-hole intersection region, while the near transducer location (position 2) looked directly at the lower surface-hole intersection region. Both transducer test positions were centered on the hole and normal to the expected direction of crack growth.

The fatigue specimens were mounted on the drilling jig for the ultrasonic test (Figure 7). The purpose of this jig was to accurately locate the specimen and the transducer wedge. The symmetry of the holes in the specimen allowed four complete tests per specimen by simply flipping and rotating

the specimen in the jig. The four tests per specimen were treated independently in the feature extraction and damage prediction analysis described later.

The plexiglas wedge carrying the transducer rode on a track on the drilling jig. Two stops on this track located the transducer at the desired near and far positions to inspect the hole. Once positioned a deadweight was placed on top of the wedge.

This testing system dictated the alignment of the transducer and the flaw and avoided deliberate operator cocking of the transducer to increase the response from a particular flaw. Removing the operator from the test variables was not completely achieved, however, as he applied the mineral oil couplant between the transducer and the wedge and the wedge and the aluminum specimen. With experience it was possible for the operator to recognize and correct "strange" amplitude time signals due to inadequate or excessive couplant.

Transducer/Plexiglas Wedge System

While the ultrasonic test was designed to be simple, the selection of the transducer and the angle of the wedge to produce a shear wave can not be done casually. The Aerotech 10 MHz, 1/4 in. dia. gamma transducer transmitted enough energy at a high frequency and sufficient band width to be reasonably expected to be sensitive to a tight crack and perhaps those changes which occur prior to actual crack formation. A larger bandwidth more highly damped transducer was considered but found to transmit insufficient high frequency energy. A

higher frequency should be considered in future work but was not used here due to amplifier limitations. Transducer characteristics are outlined in Appendix A.

The plexiglas wedge of 38.3° was chosen to produce a 45° shear wave in the aluminum based upon energy distribution calculations by Mayer [33]. These results are summarized in Figure 8. At or near the angle chosen three beneficial effects occur:

1. The shear wave carries all the energy transmitted to the aluminum.

2. The amount of transmitted energy is high (45%) with respect to the transducer energy. For the materials involved the maximum is about 48%.

3. The energy contained in the longitudinal wave reflected from the plexiglass-aluminum interface is small (2%). This is important as this energy can cause spurious signals as it reflects within the plexiglas and is eventually sensed by the transducer.

Test Equipment

A block diagram of the ultrasonic test equipment is shown in Figure 9. Studies were done to determine the operating characteristics and best combinations of settings to be used in this experimental series. The major conclusions of this work are:

1. The maximum sensitivity ($\pm$ .05V range) of the analog to digital converter should be used in conjunction with appropriate pulser-amplifier attentuation to achieve maximum

quantum level (+127 to -128) outputs of the A/D converter without overdriving it.

2. The pulser damping control should be set to achieve maximum high frequency signal content.

3. Signal averaging can reduce noise [34]. For this particular test arrangement, Figure 10 depicts the decrease in the noise (increase in signal to noise ratio) as the number of times a signal is averaged increases. This signal to noise ratio was calculated as the $\log_{10}$ of the peak signal squared divided by the variance of the signal in a "noise window." This noise window was taken as a portion of the recorded data where no information from the hole was expected to be present. In addition to improving the signal to noise ratio, there is an advantage in working with an average signal over a single digitized signal. The triggering of the A/D converter produces an uncertainty of one sample interval, thus for a given signal either side of a peak may be sampled, thus truncating it. The data recorded in this study is an average of eight signals and has a signal to noise ratio in the 45-50 DB range.

4. Since it has been found that pattern recognition algorithms are sensitive to transducer characteristics [35], a transducer acceptance check based on one used by Raisch [27] was used. This check involved comparing the signal from a hole in an unfatigued specimen that was averaged 64 times and stored in the computer to a single signal from the same specimen at the start of each testing period. The reference and single signals were cross correlated and the sum of the

squared point by point difference calculated (Figure 11). Experience has shown a sum of less than 25 to be acceptable. This check, in addition to being sensitive to transducer condition, also served as a check on the entire experimental arrangement. Misadjustment of the pulser damping control would produce a sum of about 160, and system triggering problems would produce a summed error up to 6.8×10^4.

5. A DC offset is present in most signals. This is partly due to the exponential decay of the excitation pulse to the transducer. The signals in this study were computer adjusted to a zero mean signal. The assumption of a zero mean signal was checked and found to be valid.

Typical Test Sequence and Output

A typical test sequence is illustrated in Figures 12 and 13. The described sequence assumes that the instrumentation has been properly set and that a transducer acceptance check has been made.

After manually setting the transducer in one of its eight positions and selecting an appropriate time delay to capture the signal of interest, a computer program is called. This program automatically initiates the A/D recording of the signal, its transfer to the computer, plotting the signal on the display terminal, and storing it for later analysis. The captured signals are 300 sample intervals or 3 μ sec. in length. Each signal is averaged eight times and as each of the eight is transferred to the computer it is displayed superimposed over previous signals of the set on the terminal face

as illustrated in Figure 12. This process allows the rejection of obvious spurious results.

If acceptable, the averaged RF signal and its Fourier transform are presented on a second display (Figure 13). Also displayed are the maximum and minimum A/D quantum levels to insure against overdriving. For maximum sensitivity these levels are kept in the 110 - 120 range. The offset records the number of quantum levels required to adjust the signal to a zero mean. Assuming the quantum level is acceptable a seven digit test code, described in Appendix B, is entered. This stores the data on whatever device selected. Floppy disc storage was used in this study. A data echo check is then performed to insure accurate data storage. This involves re-entering the data code and results in the RF signal being superimposed on the previous RF plot.

Following this a noise window is selected and the signal to noise ratio is calculated. Other data, particularly the amplifier attenuation (DB level), or comments are recorded on this permanent record as required. This entire process takes approximately 90 seconds.

ANALYSIS PROCEDURE

Introduction

A variety of pattern recognition techniques exist [36] and have recently been applied to nondestructive test problems by Rose [25], Mucciardi [15, 26], and Raisch [27]. Certain of these techniques, such as the minimum distance classifier, the fuzzy logic technique, and the Fisher linear discriminant are more appropriately applied to class discrimination problems rather than the goal here of developing a continuous quantitative prediction. The adaptive learning network, which is basically a multi-variate curve fit involving selection of both the variables and the coefficients, was used in this stidy since it is easily geared to a continuous prediction. Details important to the analysis and fitting of the data generated in this study follow.

Advantages of a Computer Based System

A computer based test system is required to handle the volume of data generated in this type of study and to quickly process the signal information. Such a system also provides unbiased handling of the data and thus promotes inspector objectivity.

Feature Selection

A feature is some characteristic of the signal or the transform of the signal. The entire set of features selected for every inspection is called a feature vector and serves as the list of variables considered by the adaptive

learning network (ALN). Any criteria may be used to select a feature. They may be statistical in nature, based upon a knowledge of the physical process, or arbitrarily chosen. This study selected the 53 features listed in Table 3 from the RF signal, the power spectrum of the signal, and the power cepstrum of the signal. The features were chosen because they were thought to be physically reasonable and could be easily computer selected, or because they were readily available since they were used in determining or ranking other features (such as spectral depression depths).

It should be noted that the features selected are not particularly sensitive to signal amplitude. The amplitude of a signal reflected from a crack has been shown to depend on the stress applied to the structure during the ultrasonic inspection [13]. Also, the peak amplitudes of the signals used in this study were nominally the same since the amplifier was adjusted to produce signals falling in the same A/D quantum range.

It was assumed that multiple cracks would start at the through hole and propagate across the plate. The transducer was located normal to the expected crack and centered on the hole. Thus the first reflected energy to the transducer should emanate from the leading edge of the hole followed by a superposition from the crack/damage region (Figure 14). As the crack grows in depth and length the amount of energy in this superimposed signal should increase and the superposition should tend to occur over a larger and later time band.

Whaley and Adler [21, 37] have shown the ability to determine the size and orientation of an immersed smooth flaw based upon a frequency analysis of the return signal. This was based on the interference of the energy scattered from the edges of the flaw while the spectral reflection from the flaw was not directed to the transducer. This study anticipated a superposition from the hole and the flaw. However, since the transducer was nominally normal to the crack and the crack was expected to form on the plate surface, the superimposed signals would originate from scattered energy from flaw edges and the spectral reflection from the flaw surface. In addition the expected rough crack surface and variations in the crack closure were expected to further distort the spectral analysis.

The cepstrum transform is summarized in [38]. The power cepstrum, which is defined as the absolute value of the Fourier transform of the log of the power spectrum, provides indications of the amplitude and arrival time associated with delayed and superimposed echos.

Representative amplitude time, spectrum, and cepstrum signal representations are shown in Figure 15. The features listed in Table 3 involve two from the RF signal meant to sense early signal superposition, twenty-six from the spectrum meant to sense frequency shifts or distinct depressions caused by superposition effects, and twenty-five from the cepstrum, designed also to sense the effects of signal superposition.

As previously mentioned, a single test consisted of the output of two transducers located on one side of the plate.

In order that the test feature vector not be overly long for computer reasons and since only one answer was available for test correlation purposes the two feature vectors from each inspection site were added to form a test feature vector containing 53 features. Each inspection feature vector was equally weighted due to the assumed symmetric damage pattern expected from the fatigue loading. Note that some of the features were ordered in order to facilitate this addition process.

Adaptive Learning Network

The ALN is basically an automatic curve fitting process that also selects the variables (features) to be used in the fitting process. All combinations of features taken two at a time are considered in the series.

$$Y_1 = A_o + A_1X_1 + A_2X_2 + A_3X_1^2 + A_4X_2^2 + A_5X_1X_2.$$

This basic building block is represented in Figure 16. The six coefficients are selected to produce the best fit to the data.

The answers produced by a given block define a new feature which can be combined with other blocks at the next level to produce a better fit. This procedure can be repeated (Figure 16). Thus the second level produces up to a 4th order fit, the third level an 8th order fit and so on. Care must be taken that overfitting does not occur, however.

In order to select the coefficients and the best feature combinations (blocks) the data is broken into three sets, called here the training, the selection, and the test set.

A variety of procedures are available to select these sets. In this study the data was divided into four classes spanning the range of the fatigue data. Data from each class was then randomly and approximately equally placed in each ALN set. Thus each set contained 1/3 of the entire data and a given piece of data was used in only one set. This is thought to result in a rigorous test of the ALN procedure. This also requires a fairly large data base. Table 4 outlines this procedure.

The training set features and answers are used in the computer routine to select the best coefficients for each block. The selection set features are then used to select the best blocks. This can be done by using the training coefficients to predict a selection answer and comparing this to the actual selection set answers. In this study, the sum of the squared errors resulting from this comparison was used to select the best blocks. Since the 53 features resulted in 1378 first level blocks the need to severely limit the "good" blocks for input to level two is obvious. An outline of the final network is shown in Figure 17. The last step consisted of summing the results from each last level block and averaging the results.

It might be noted that disjoint blocks are possible. For example, if a good block at level one does not combine to produce good results at level two it may be sent directly to the summation step. This procedure was not used in this study since the squared error threshold used to select the best blocks

for input to the next level was made progressively tighter and because of the large number of boxes summed from level three. To be useful the squared error of a disjoint block would have to be equal to the error of a higher level block. If this were true the necessity of proceeding to a higher order fit could be questioned.

Once an entire ALN network is defined the test set, data heretofore unseen, is used to evaluate the accuracy of the developed fitting procedure.

ALN Dilemma

The following problems confront the user of an ALN procedure:

1. Has the best feature been chosen? This is never certain. All that can be said is that acceptable results have been achieved.

2. Has the threshold technique rejected a level 1 block that, if kept, would be very good at level 2?

3. Is a small amount of bad data creating such large errors that good blocks are masked and not selected?

This study used a standard selection procedure based on the sum of the squared errors for all data in the selection set. A sum squared error of $.2 \times 10^5$, for example, is equivalent to an average error of $\pm$ 19 for each of the 55 set points. This procedure resulted in the selection of 9 of the 53 original features. These nine are shown in Figure 17 and are features 46, 28, 6, 11, 25, 29, 36, 37, and 49.

However, in order to attack Problems 2 and 3 mentioned above a second procedure, given the name "opportunity analysis", was developed. While its results were similar but not superior to the squared error approach, and thus not reported, the process may be valuable in other work.

The basis of the opportunity analysis is the idea that each feature had 52 chances to combine with another feature and better a particular threshold. It is assumed that the best features will better this threshold most often. A high threshold was set to avoid the problem of masking and all the features ranked by the number of times they were selected. This resulted in a subset of 16 features (46, 28, 36, 6, 43, 11, 33, 37, 49, 48, 53, 4, 42, 45, 51, and 50). Also a seventeenth feature, the constant 1, was added to this group to see if single features were capable of solving the problem. This smaller set of features was then run through the ALN with less stringent early level squared error thresholds, thus allowing more blocks to reach the second level.

While this procedure did not improve results it did partly confirm the 9 features actually used and produced a feature subset that was physically realistic.

FRACTURE MECHANICS CONSIDERATIONS

This study was based upon the quantification of fatigue damage and not the measurement of a crack dimension per se. Figure 1 illustrates the motivation for finding ever smaller flaws. As the detectable flaw size is reduced (Ai vs. Al) an increase in structure lifetime or allowable stress is produced. Since most previous studies have looked at the detection or measurement of crack length a comparison of the two approaches is useful.

Appendix C outlines a fracture mechanics procedure which indicates that for a specific set of material, geometry, and loading conditions the cycles to failure is primarily dependent upon the size of the initial crack sensed.

$$N_f = K \left(\frac{1}{ai^{(n-2)/2}}\right)$$

Table 5 uses this procedure to relate errors in the estimation of a crack length to the resulting error in estimating the number of cycles to failure. Note that errors in estimating crack lengths from $\pm$ 10% to $\pm$ 60% result in underestimations of fatigue life from 13% to 52% and overestimations of fatigue life, the more dangerous situation, from 17% to 295%.

CRACK MORPHOLOGY

A study was conducted to estimate the crack sizes and shapes in the vicinity of the detection limit. Three specimens were fatigue loaded to 10%, 20%, and 30% of their expected lifetimes based upon the mean life of previous specimens. The specimen surfaces were examined in a metallograph at a magnification of 100. Photographs of the surface-hole intersection area where cracks formed are shown in Figure 18. Table 6 summarizes the size of the cracks found using this procedure. Positions 1 through 4 are the four intersection points.

Following the surface examination, the specimens were axially loaded to failure. This produced a fracture surface where the fatigue region was clearly indicated. Photographs of this fracture surface made on a scanning electron microscope (SEM) appear in Figure 19. Flaw dimensions from these photographs appear in Table 7.

Figure 20 illustrates typical fracture surfaces for those specimens failed in the fatigue test. Note the variations in surface roughness and the symmetry of the failure surfaces.

From this entire series of photographs it is observed that:

1. The fatigue damage was not always symmetrically distributed between the top and bottom of the specimen.

2. The early cracks tended to follow grain boundaries and were not normal to the longitudinal axis of the specimen.

3. The crack propagation involved various amounts of shear contribution.

It is expected that these variations contribute to the error and scatter evident in the prediction results.

To further illustrate the problems of basing an analysis upon signal amplitude, amplitude-time signals for these three specimens prior to fatigue loading (0%) and following fatigue loading are compared in Figure 21. The transducer location was identical for each pair of signals. Almost no difference can be detected between the signals after 10% or 20% fatigue life. Some differences exist for the 30% case. However, since a 0% damage baseline for each possible fatigue site is not practical it is necessary to develop a procedure to distinguish the 0% signal for the 30% specimen from the 20% signal.

RESULTS

An ALN procedure utilizing 9 features from the spectrum and cepstrum transforms of an ultrasonic signal was used to detect and measure fatigue damage. Detection of specimens having undergone greater than 10% of the fatigue life was made 92% of the time. Estimation of the actual damage level expressed as percent fatigue life experienced was made to within $\pm$ 20 of the actual value for 76% of the tests. The prediction results for the training, selection, and test data sets are shown in Figures 22, 23, and 24. Table 8 outlines the results depicted in the above figures. Table 9 outlines the detection results.

As expected the training and selection sets yield better prediction results than the test set. This is indicated by comparing the squared errors for each set in Table 8. However, the squared error for the test set is reduced to $.172 \times 10^5$ if the obviously erroneous predictions of 317 and -144 for actual values of 32 and 95 are neglected. This is then the same order as the other sets. While the predictions for all the data sets is included in Table 8, only the test set provides a realistic evaluation of the potential of this process.

Threshold levels can be set to use the ALN predictions as a class identifier. "Damage" - "No Damage" thresholds at predictions of 10% and 20% produced the reliabilities outlined in Table 9. A point was considered correctly classified if it was within the threshold or within $\pm$ 10 of its actual value.

Misclassification can have two consequences. Classifying "damage" as "no-damage" can have catastrophic results while classifying "no-damage" as "damage" can have costly but not catastrophic effects. As one would expect, as this threshold is lowered more damage data is correctly classified.

Two concerns surface in this work. First, while the developed ALN procedure is fairly good at detecting and estimating small amounts of fatigue damage it fails to accurately predict large amounts of damage - a supposedly easier problem. This may be due to the fact that more data was taken in the more critical low damage region. Also, due to the size of the transducer diameter and the through hole diameter, the ultrasonic test may have been less sensitive to the larger cracks corresponding to the high damage data. A third possibility is that the cepstrum procedure was not sensitive to large cracks. An assumption in the cepstrum procedure is that the amplitude of the time-delayed signal is less than that of the main (hole) signal. If this is not the case the series expansion used breaks down. The second concern involves the gross misestimation of two points in the test set. This indicates that the feature vectors for these points are outside the trained range. A "no test" decision step in the ALN procedure could solve this problem. Perhaps such unrealistic answers are an extreme "no test" decision themselves.

CONCLUDING REMARKS AND RECOMMENDATIONS

1. The ability of advanced signal gathering and analysis to solve a detection and estimation problem involving a difficult and realistic flaw type has been demonstrated. The concept of measuring damage rather than some specific flaw parameter may be generally useful.

2. Procedures to best use available instrumentation and inspection techniques coupled with signal analysis have been illustrated. It is thought that eventually the results of a study of this type, such as the features found to be important, can be incorporated in a feedback loop affecting equipment requirements, test techniques, and the analysis procedure.

3. Some problems associated with the ALN were outlined. A study of the effects of variations on this procedure with the aim of improving or optimizing it would be beneficial.

4. The requirements of transducer/test acceptance need to be better defined. Also, the ability to transform the results from one transducer, set of test conditions, type of loading, material, etc. to other similar conditions would be extremely useful. At a minimum, it is expected that as a variety of problems are solved sets of features will emerge that define solutions to certain classes of problems.

LIST OF REFERENCES

LIST OF REFERENCES

1. Feltham, P., "The Origin of Defects in Solids - Part 2". Non-Destructive Testing, April 1970, pp. 105-110.

2. Dieter, G.E., Jr., Mechanical Metallurgy, McGraw-Hill, New York, 1961.

3. Rummel, W.D. et al, "The Detection of Fatigue Cracks by Nondestructive Testing Methods", NASA CR-2369, February 1974.

4. Schroeer, R., "Research on Exploratory Development of Nondestructive Methods for Crack Detection", AFML-TR-67-167.

5. Birchak, J.R. and Gardner, C.G., "Comparative Ultrasonic Response of Machined Slots and Fatigue Cracks in 7075 Aluminum", Materials Evaluation, December 1976, p. 275.

6. Silk, M.G., "Accurate Crack Depth Measurements in Welded Assemblies", Proceedings of the Eighth World Conference on Nondestructive Testing (2B16), September 1976.

7. Funke, G. and Pawlowski, Z., "Acoustic Emission and Fractographic Analysis Applied to the Estimation of Crack Growth During Low-Cycle Fatigue", Proceedings of the Eighth World Conference on Nondestructive Testing (3K10), September 1976.

8. AFSC Design Handbook Series 1 - 0 - General Design Factors, AFSC DH 1-2, DN7A1, 3rd ed. February 1974.

9. Packman, P.F., Pearson, H.S., Owens, J.S., and Young, G., "Definition of Fatigue Cracks Through Nondestructive Testing", J. of Materials, JMLSA, vol. 4, no. 3, September 1969, pp. 666-700.

10. Papadakis, E.P., "Future Growth of Nondestructive Evaluation" IEEE Transactions on Sonics and Ultrasonics, vol. su-23, no. 5, September 1976, pp. 284-287.

11. Worlton, D.C., Frederick, C.L., and Denton, C.J., "Recent Advances in Nondestructive Testing Technology at Hanford", J. of Materials, vol. 1, December 1966, pp. 809-822.

12. Albertini, C., and Basile, D., "Statistical Evaluation of the Results of Nondestructive Tests Carried Out on SAP Reactor Pressure Tubes", Materials Evaluation, vol. 28, August 1970, pp. 182-188.

13. Corbly, D.M., Packman, P.F., and Pearson, H.S., "The Accuracy and Precision of Ultrasonic Shear Wave Flow Measurements as a Function of Stress on the Flaw", Materials Evaluation, May 1970, pp. 103-110.

14. Raatz, C.F. et al, "Detection of Cracks Under Installed Fasteners", AFML-TR-74-80, April 1974.

15. Shankar, R., Mucciardi, A.N. et al, "Adaptive Nonlinear Signal Processing for Characterization of Ultrasonic NDE Waveforms, Task 2: Measurement of Subsurface Fatigue Crack Size", AFML-TR-76-44, April 1976.

16. Green, R.E., Jr., and Pond, R.B., Sr., "Ultrasonic Detection of Fatigue Damage in Aircraft Components" AFOSR-TR-77-658, March 1977.

17. Joshi, N.R., and Green, R.E., Jr., "Ultrasonic Detection of Fatigue Damage", Engineering Fracture Mechanics, vol. 4, 1972, pp. 577-583.

18. Krautkramer, J., and Krautkramer, H., Ultrasonic Testing of Materials, Springer-Verlag, New York, 1969.

19. Rose, J.L., Mortimer, R.W., and Chou, P.C., "Applications of Dynamic Photoelasticity in Flaw Detection Analysis", Materials Evaluation, vol. 30, no. 11, pp. 242-247.

20. Gericke, D.R., "Ultrasonic Spectroscopy", Chapter 2 in Research Techniques in Nondestructive Testing, ed. by R.S. Sharpe, Academis Press, 1970, pp. 31-61.

21. Whaley, H.L., and Adler, L., "Flaw Characterization by Ultrasonic Frequency Analysis", Materials Evaluation vol. 29, August 1971, pp. 182-188.

22. Rose, J.L., Carson, J.M., and Leidel, D.J., "Ultrasonic Procedures for Inspecting Composite Tubes", ASTM STP 551, American Society for Testing and Materials, Philadelphia, 1973, pp. 311-325.

23. Ermolov, I.N. et al, "Flaw Shape Discrimination in Ultrasonic Testing" (3H8) proceedings of the Eighth World Conference on Nondestructive Testing, September 1976.

24. Nabel, E., and Newmann, E., "Evaluation of Flaw Indications by Ultrasonic Pulse Amplitude and Phase Spectroscopy" (3H6) Proceedings of the Eighth World Conference on Nondestructive Testing, September 1976.

25. Rose, J.L., "A 23 Flaw Sorting Study in Ultrasonics and Pattern Recognition", Materials Evaluation, July 1977, pp. 87-92.

26. Mucciardi, A.N. et al, "Adaptive Nonlinear Signal Processing for Characterization of Ultrasonic NDE Waveforms, Task 1 - Inferences of Flat-Bottom Hole Size". AFML Interim Report, Contract Number F33615-74-C-5122.

27. Raisch, J.W., "An Automated Computer Controlled Ultrasonic Adhesive Bond Evaluation Technique", Ph.D. Thesis, Drexel University, June 1977.

28. Tiffany, C.F., Stewart, R.P., and Moore, T.K., "Fatigue and Stress-Corrosion Test of Selected Fasteners/Hole Processes", ASD-TR-72-211, Wright Patterson AFB OH, 1973.

29. Gran, R.J., Orazio, F.D., Paris, P.C., Irwin, G.R., and Hertzberg, R., "Investigation and Analysis Development of Early Life Aircraft Structural Failures", AFFDL-TR-70-1439, Wright Patterson AFB OH, 1970.

30. Popov, E.P., Mechanics of Materials, Prentice Hall, Englewood Cliffs, NJ, 2nd Ed., 1976.

31 Swanson, S.R., Handbook of Fatigue Testing, ASTM STP 566, American Society for Testing and Materials, Philadelphia, 1974.

32. Graham, J.A. ed., Fatigue Design Handbook, Society of Automotive Engineers, Inc., New York, 1968.

33. Mayer, W.G., "Energy Partition of Ultrasonic Waves at Flat Boundaries", Ultrasonics, April-June 1965, pp. 62-68.

34. Schwartz, M., and Shaw, L., Signal Processing, McGraw-Hill, New York, 1975.

35. Rose, J.L., and Avioli, M.J., "Transducer Compensation Concepts in Flaw Classification" presented at the Spring ASNT Conference, New Orleans, April 1978.

36. Duda, R.O., and Hart, P.E., Pattern Classification and Scene Analysis, John Wiley and Sons, New York 1973.

37. Adler, L., and Lewis, K., "Models for the Frequency Dependence of Ultrasonic Scattering from Real Flaws", Proceedings of the ARPA/AFML Review of Progress in Quantitative NDE, AFML-TR-77-44, September 1977.

38. Kemerait, R.C., and Childers, D.G., "Signal Detection and Extraction by Cepstrum Techniques", IEEE Transaction on Information Theory, vol. IT-18, no. 6, November 1972, pp. 745-759.

% Fatigue Life Experienced	Local Series		Express Series	
	Spec. No.	Tests	Spec. No.	Tests
0		12		19
0 - 3			4. 21. 22	12
3 - 8			5. 15	8
8 - 13	1. 2. 3	12	6. 9. 16	12
13 - 18			20	4
18 - 25	1. 2. 3	12	10. 12. 17. 19	16
25 - 40	1. 2. 3	12		
40 - 60	1. 2. 3	12	7. 8. 18	12
60 - 80	1. 2. 3	12	11	4
80 - 100			13. 14	8
Subtotal	3	72	19	95

Total Specimens: 22

Total Inspections: 167

Table 1. Test Program

Specimen No.	Cycles to Failure
1	27,700
2	28,400
3	29,000
4	46,300
5	39,900
6	33,600
7	47,300
8	61,300
9	35,500
10	26,500
11	46,000
12	28,200
13	41,700
14	35,400
15	33,800
16	29,000
17	27,500
18	25,600
19	23,000
20	27,800
21	29,100
22	23,700

Nominal Stress = 34.0 ksi
R = -1
Mean cycles to failure: 33,900
Standard deviation: 9,600

Table 2. Fatigue Test Results

Amplitude-Time

1. first positive maximum above 20 quantum levels divided by the next positive maximum
2. first negative maximum above 20 quantum levels divided by the next negative maximum

Spectrum

3. peak frequency
4. 6 dB down bandwidth
5. 6 dB down mid-frequency

6-11. six largest frequency depressions ranked in descending order (5-15 MHz window)

12-17. frequency of six largest dips ranked by frequency (5-15 MHz window)

18-27. fractional power in 1 MHz intervals from 5-15 MHz normalized by total spectral power

28. total spectral power 5-15 MHz

Cepstrum

29-35. time of seven largest peaks ranked by amplitude

36-42. time of seven largest peaks ranked by amplitude x time product

43-52. area in 20 SI windows from 0 to 200 normalized by total cepstral area

53. total cepstral area from 0 to 200 SI

Table 3. List of Features

	FATIGUE CLASSES				
	0 - 3%	3 - 18%	18 - 35%	35 - 90 %	Total
Total Tests	43	36	40	48	167
Training Set	14	12	13	16	55
Selection Set	14	12	13	16	55
Test Set	15	12	14	16	57

Table 4. ALN Data Distribution

Crack Length (a_i) Error	Cycles to Failure (N_f) Error (n = 5)
±10%	-13 to +17%
±20%	-24 to +40%
±30%	-33 to +71%
±60%	-52 to +295%

Table 5. Fatigue Life Estimate Errors

Specimen	POSITION 1	2	3	4
10%	.03 mm .001 in	0 0	.40 mm .016 in	.30 mm .012 in
20%	.80 mm .013 in	.35 mm .014 in	.65 mm .026 in	.60 mm .024 in
30%	.90 mm .035 in	.80 mm .031 in	1.10 mm .043 in	.70 mm .028 in

Table 6. Surface Crack Sizes

Position	Specimen 10%	20%	30%
A length	.51 mm .020 in	.85 mm .033 in	2.11 mm .083 in
depth	.92 mm .036 in	1.43 mm .056 in	2.11 mm .083 in
B length	0	1.02 mm .040 in	2.21 mm .087 in
depth	0	1.29 mm .051 in	2.04 mm .080 in
C length	.44 mm .017 in	.85 mm .033 in	1.65 mm .065 in
depth	.68 mm .027 in	1.19 mm .047 in	1.80 mm .071 in
D length	.49 mm .019 in	1.22 mm .048 in	1.46 mm .057 in
depth	.78 mm .031 in	1.48 mm .058 in	1.90 mm .075 in

Table 7. Crack Dimensions from Fracture Surface Indications

Set	Sq. Error x 10^5	% Data Within ±10	±20	±30
Training	.114	54.5	85.5	96.4
Selection	.128	61.8	89.1	96.4
Test	1.56 (.172)	58.2	76.4	85.5
Total		58.2	83.6	92.7

Table 8. Fatigue Estimation Results

Threshold	Set	% Correctly Classified No Cracks (<T)	Cracks (>T)
20	Training	93.3	92.0
	Selection	86.2	100
	Test	88.5	72.4
	Total	89.4	87.5
10	Training	78.9	97.2
	Selection	90.0	100
	Test	83.3	91.9
	Total	84.2	96.3

Table 9. Fatigue Detection Results

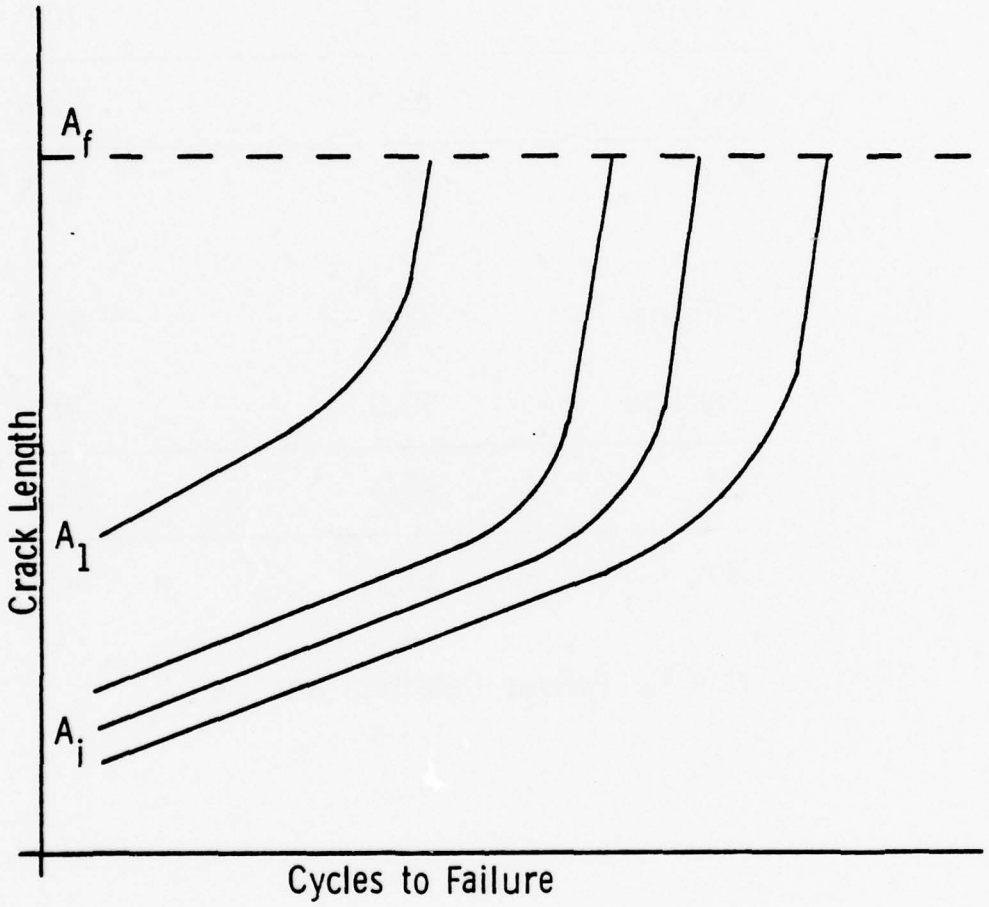

Figure 1. Crack Size Related to Fatigue Life

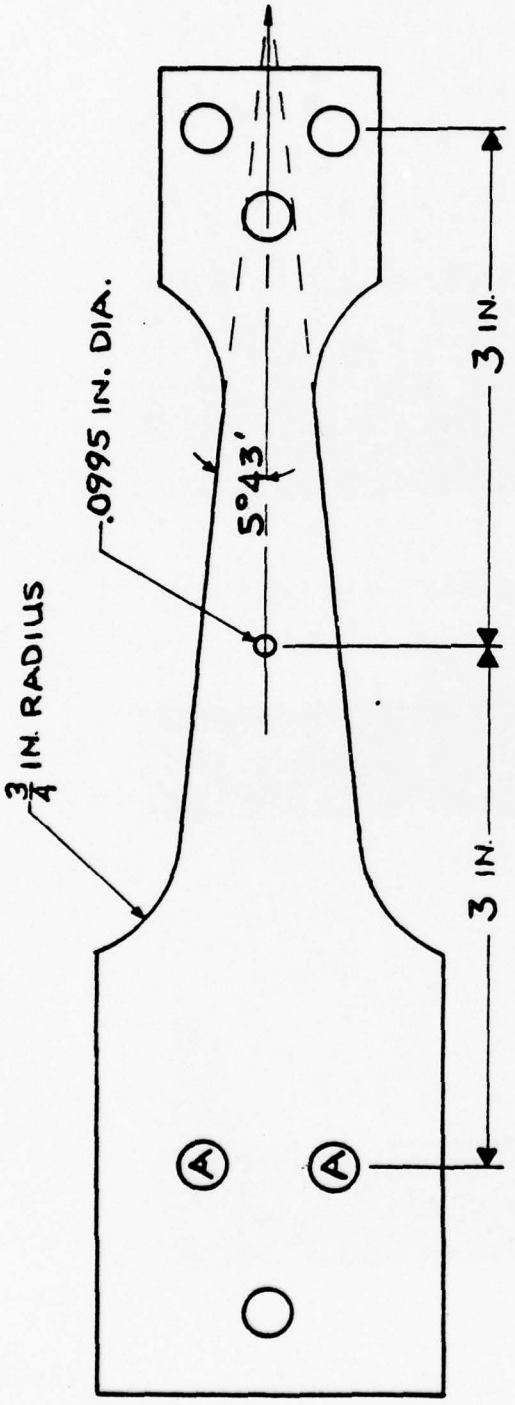

Figure 2. Fatigue Test Specimen

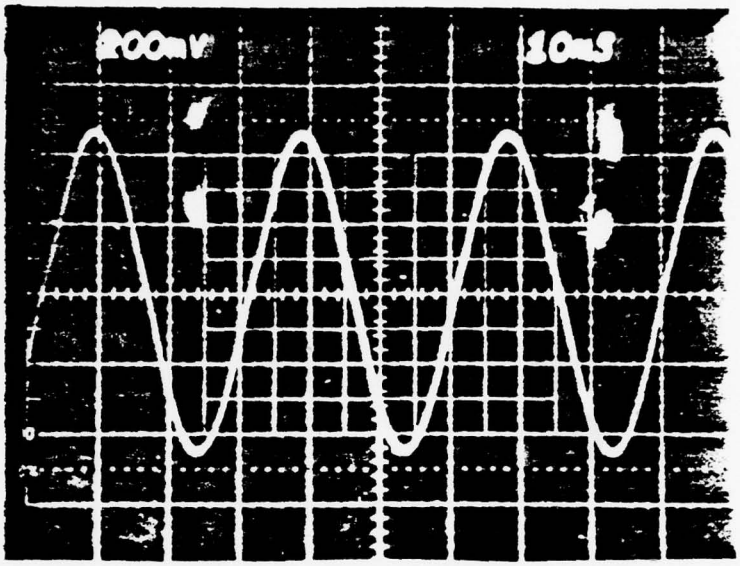

Figure 3. Fatigue Testing Rate (2000 cycles/min)

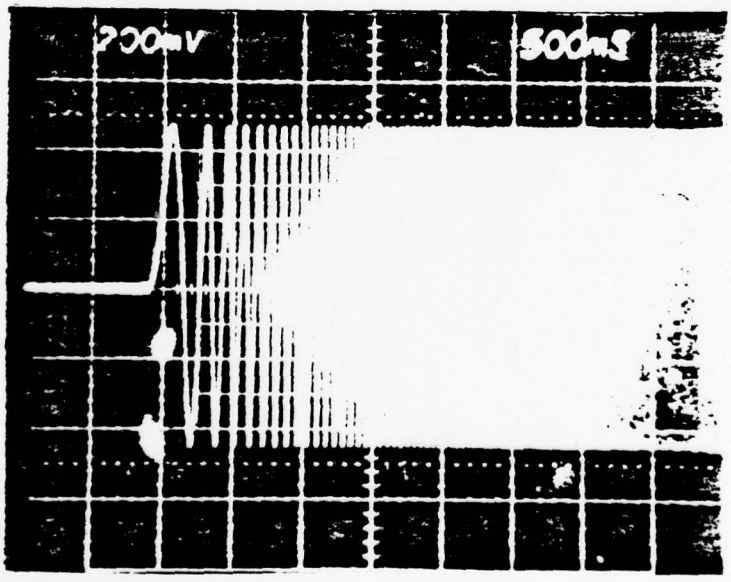

Figure 4. Fatigue Test Start Up (500 ms/div)

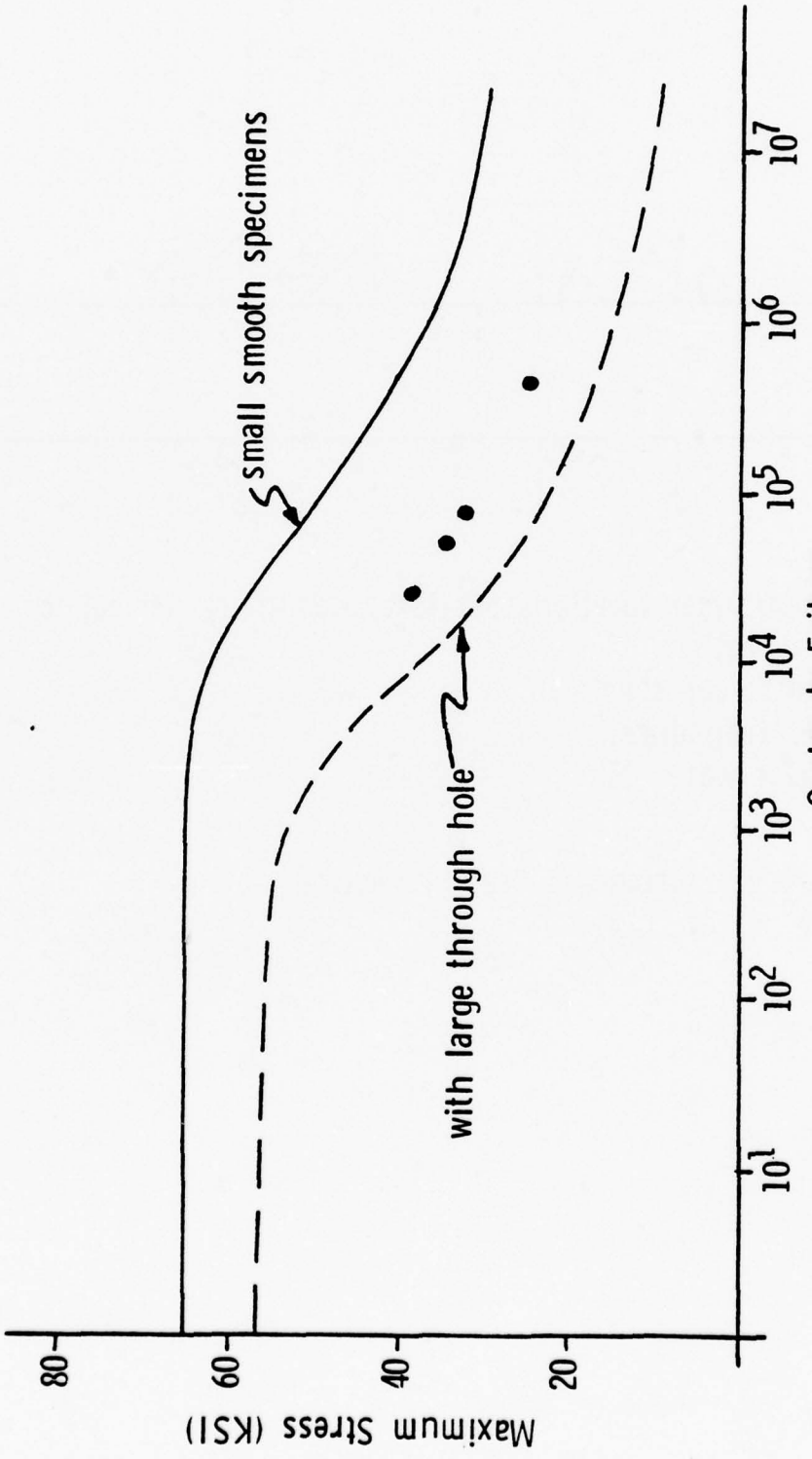

Figure 5. Comparison of Fatigue Data

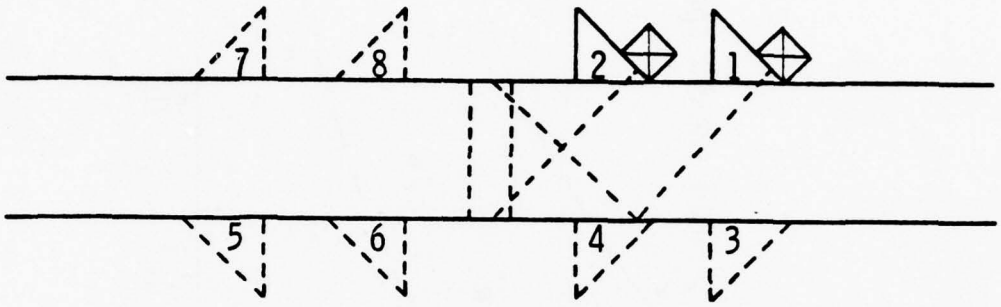

- two transducer locations per test, nominally normal to crack direction
- four tests per specimen
- 10 MHz transducer
- 45° shear wave

Figure 6. Ultrasonic Test Procedure

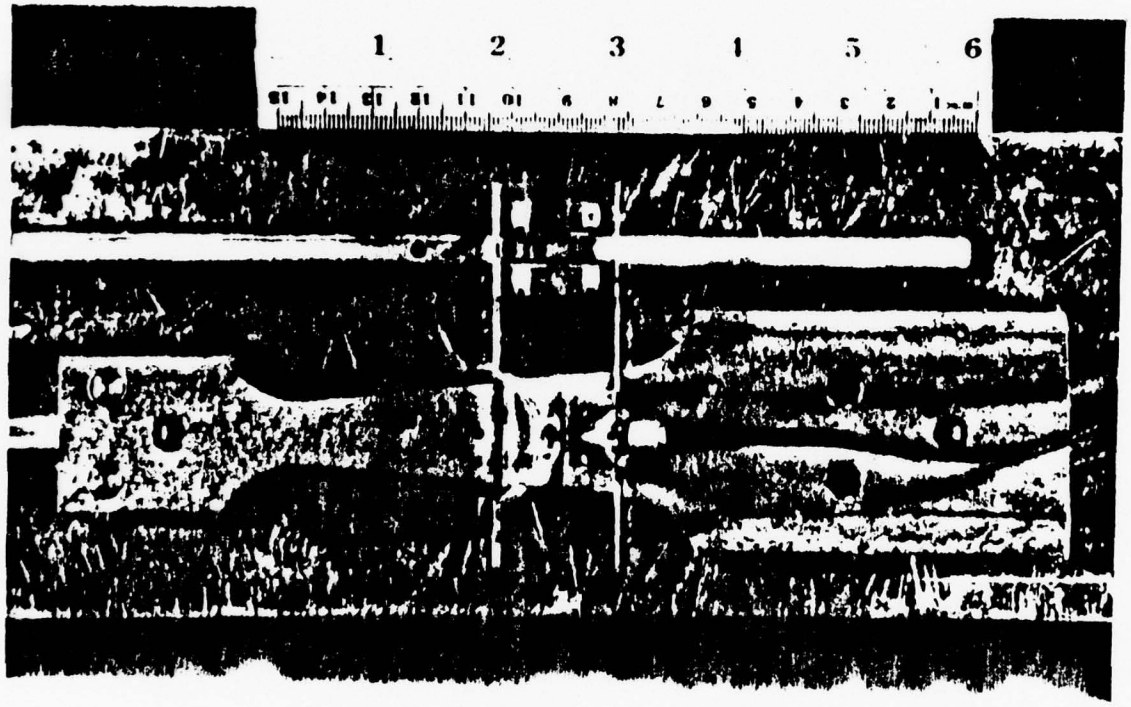

Figure 7. Ultrasonic Test/Drilling Jig

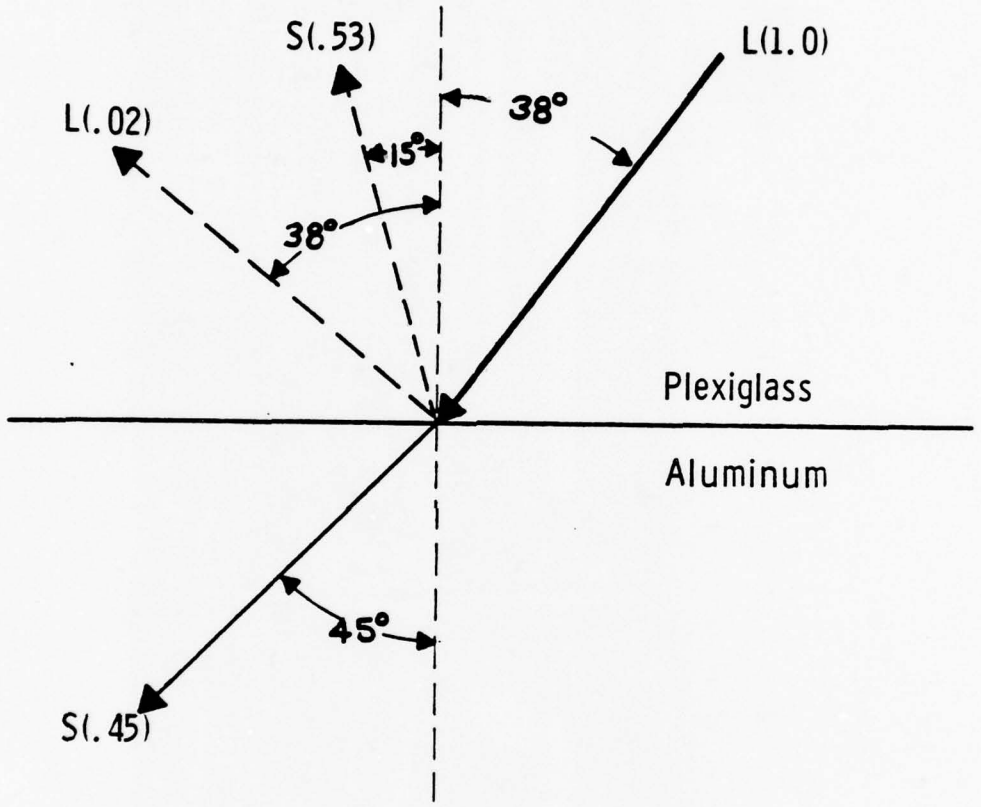

Figure 8. Distribution of Incident Energy (L = 1.0)

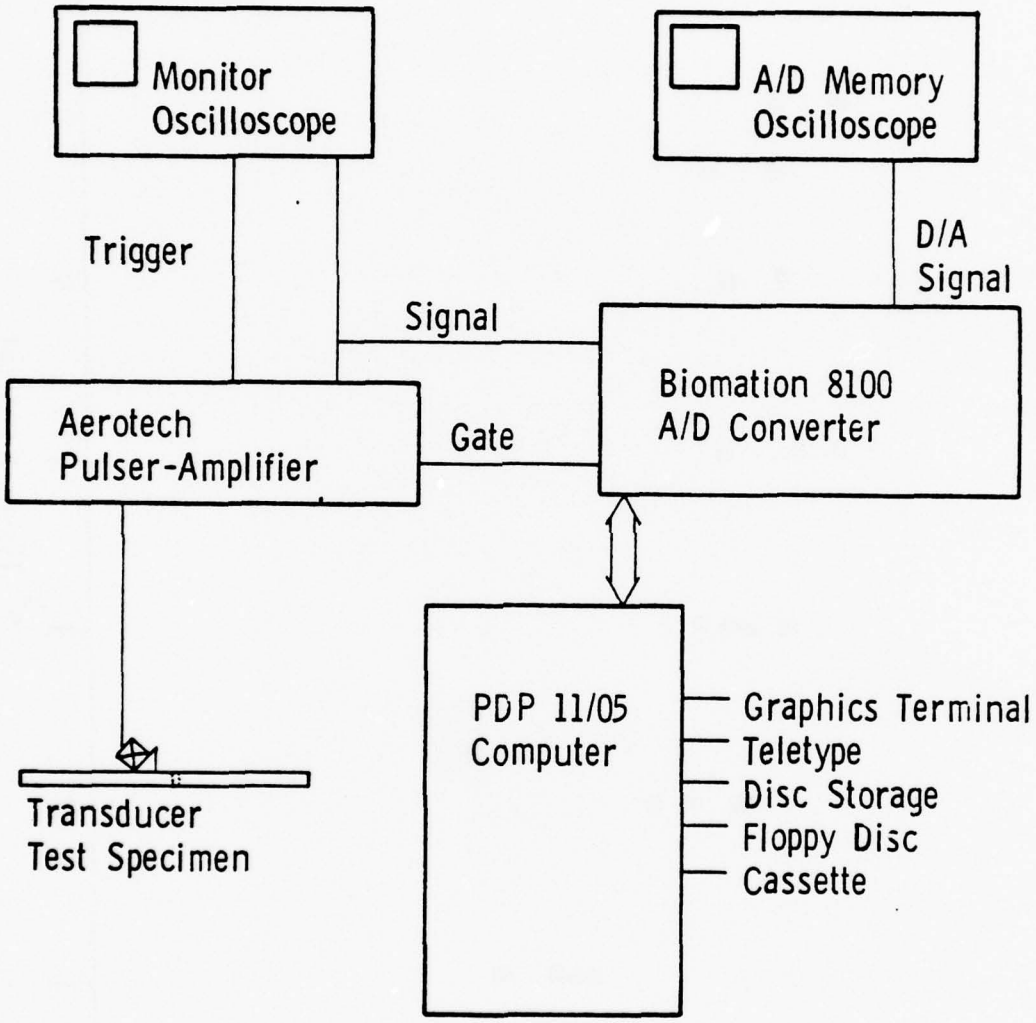

Figure 9. Diagram of Test Equipment

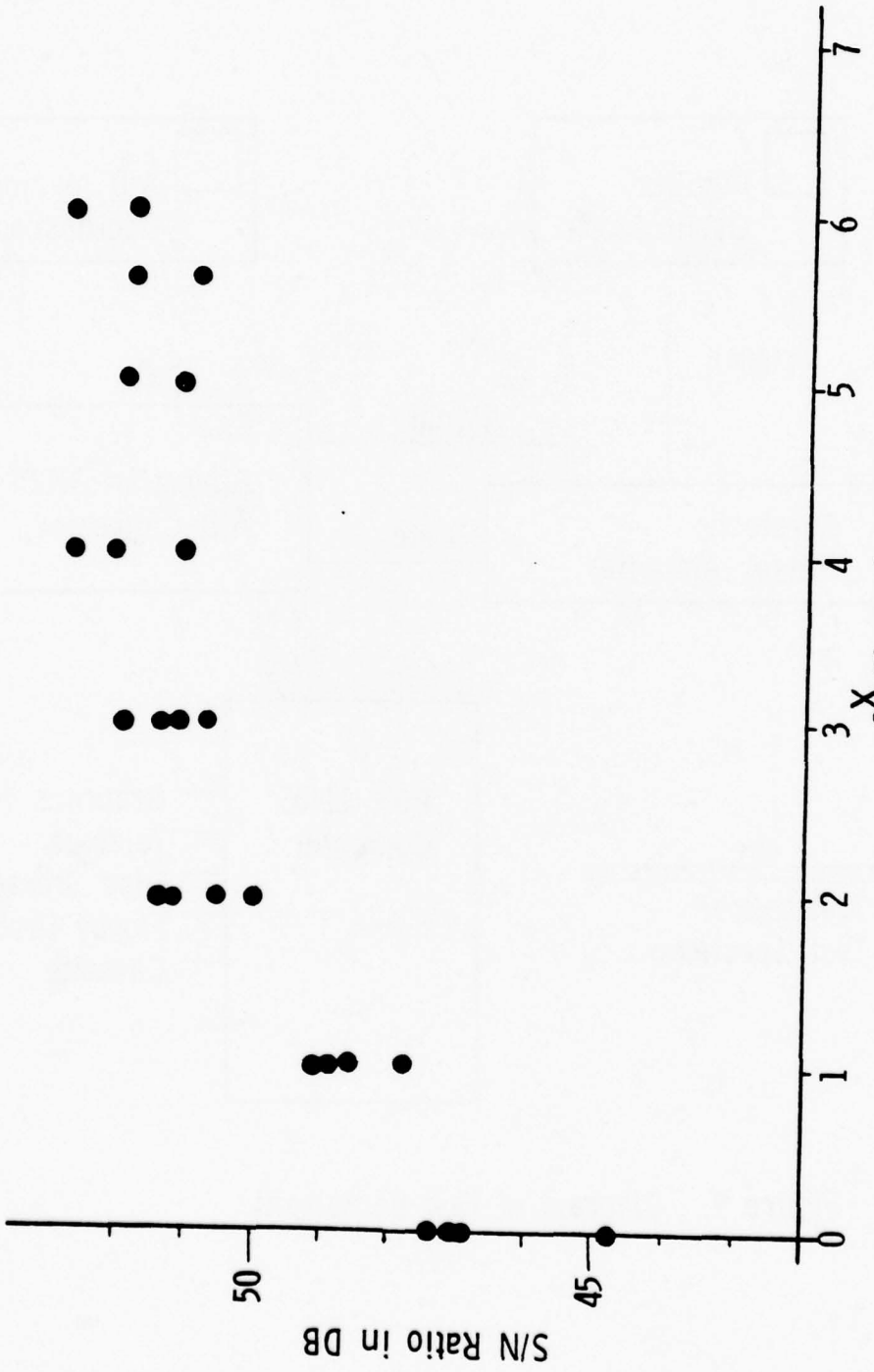

Figure 10. S/N Ratio vs. Times Averaged

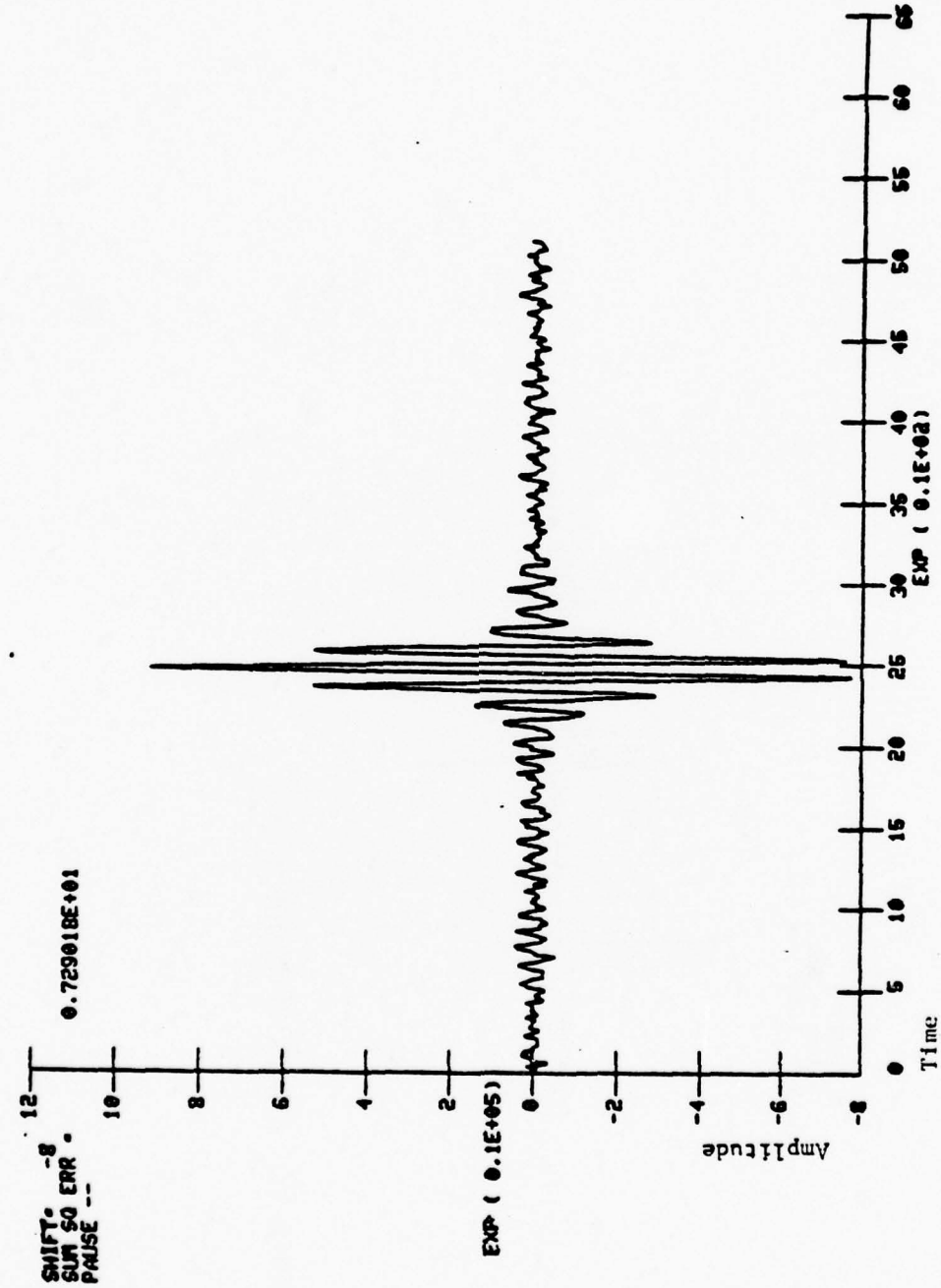

Figure 11. Transducer Acceptance Check

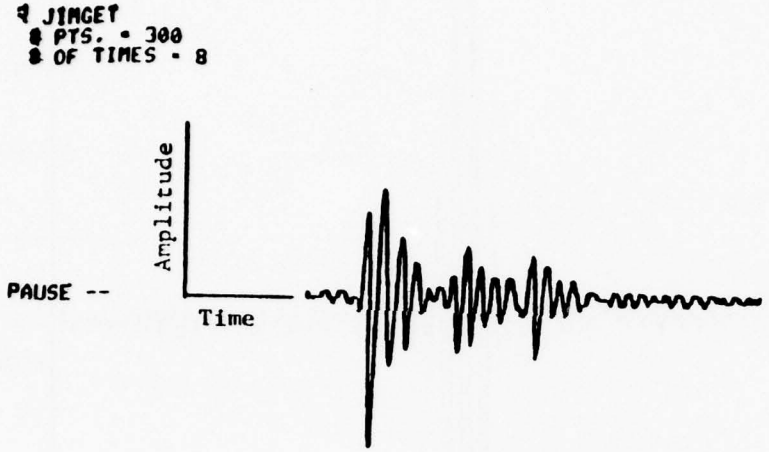

Figure 12. Check of Input Data

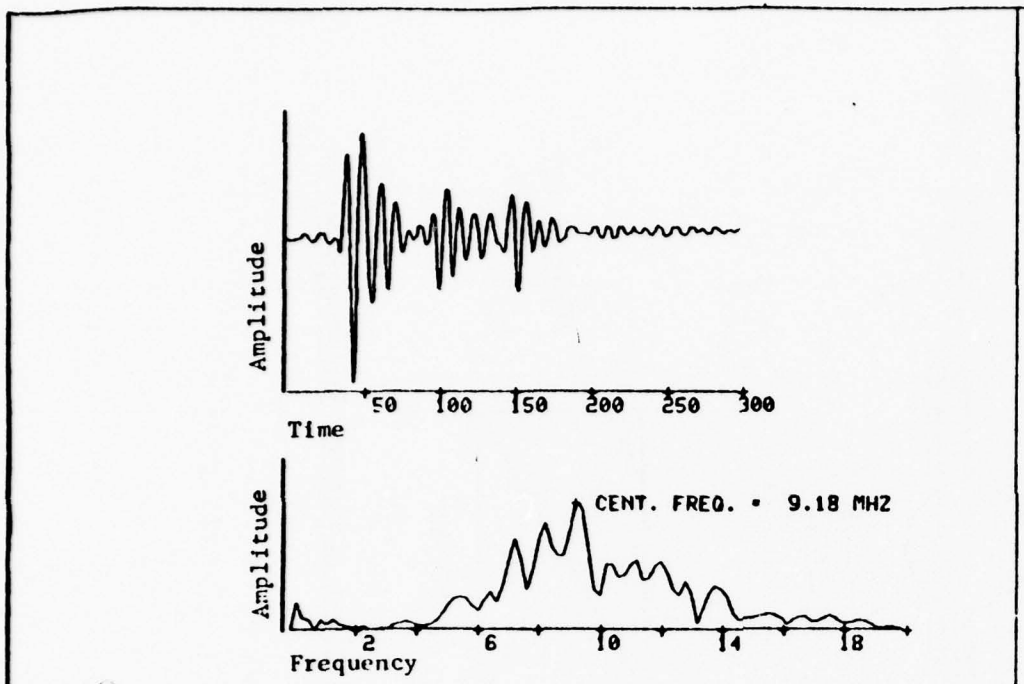

COMMENTS

# PTS	• 300	DB LEVEL	• .....
# OF TIMES	• 8	REP RATE	• .....
MAX Q LEVEL	• 48	# OF CYCLES	• .....
MIN Q LEVEL	• -121		
OFFSET	• -20		

NOISE WINDOW
200
300

SIG/NOS • 38.12 DB

TEST CODE - #
CHECK - #

Figure 13 - Data Output Format

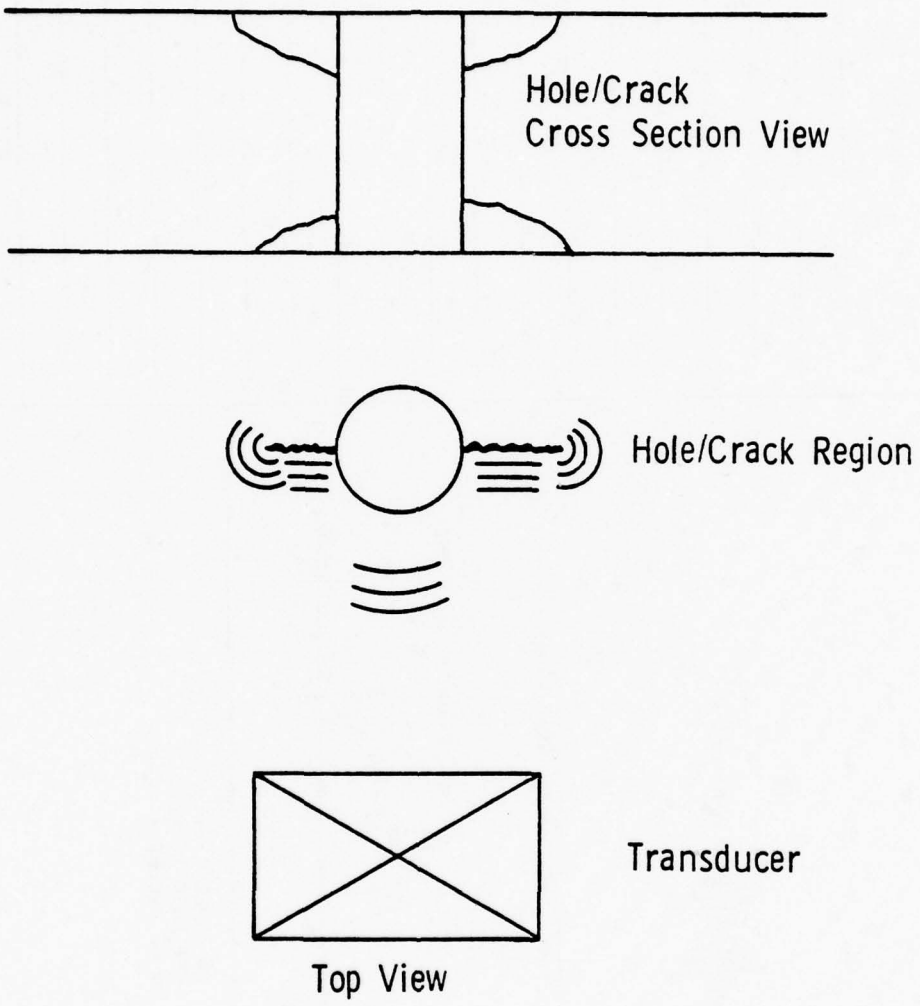

Figure 14. Illustration of Signal Superposition

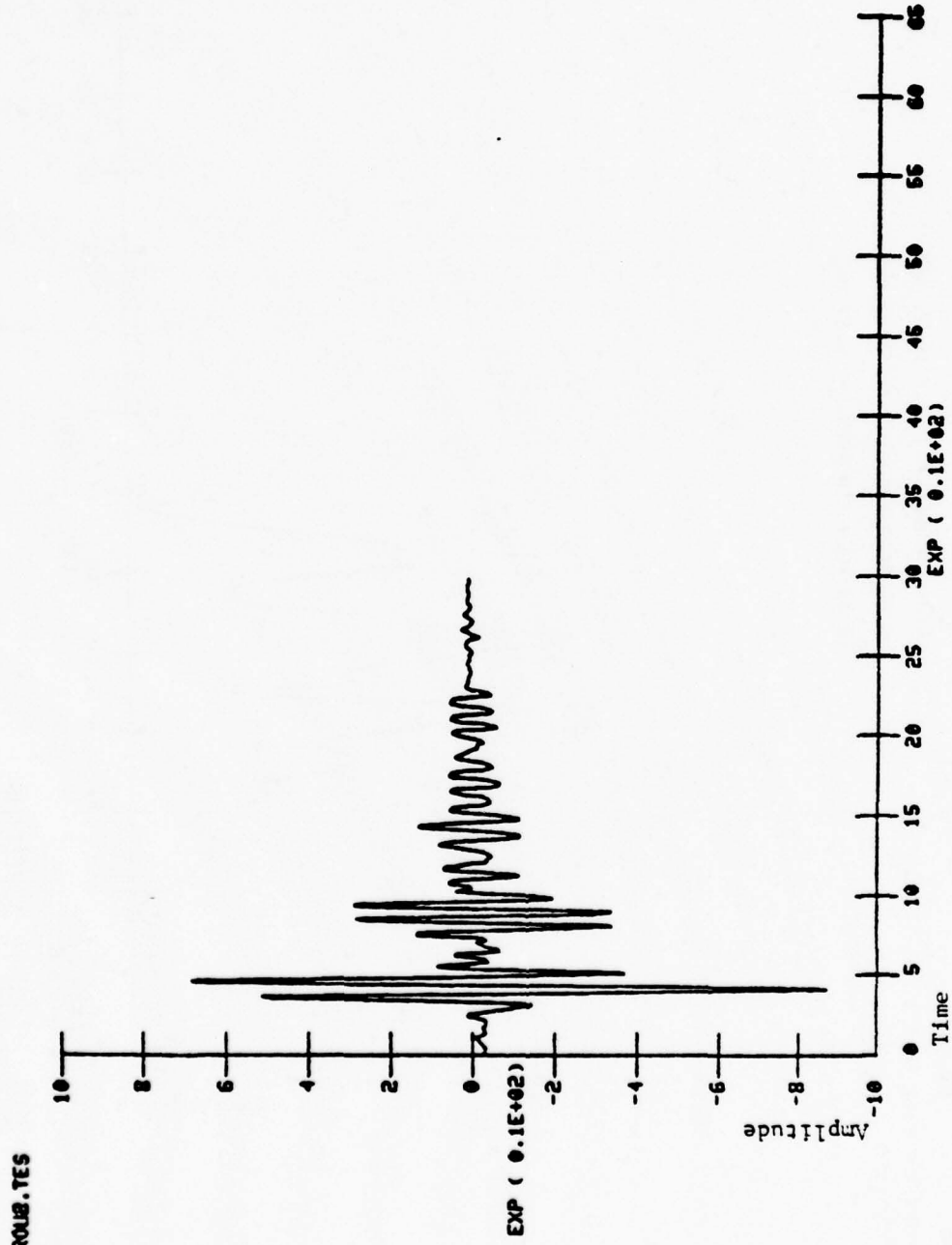

Figure 15A. Signal Amplitude-Time

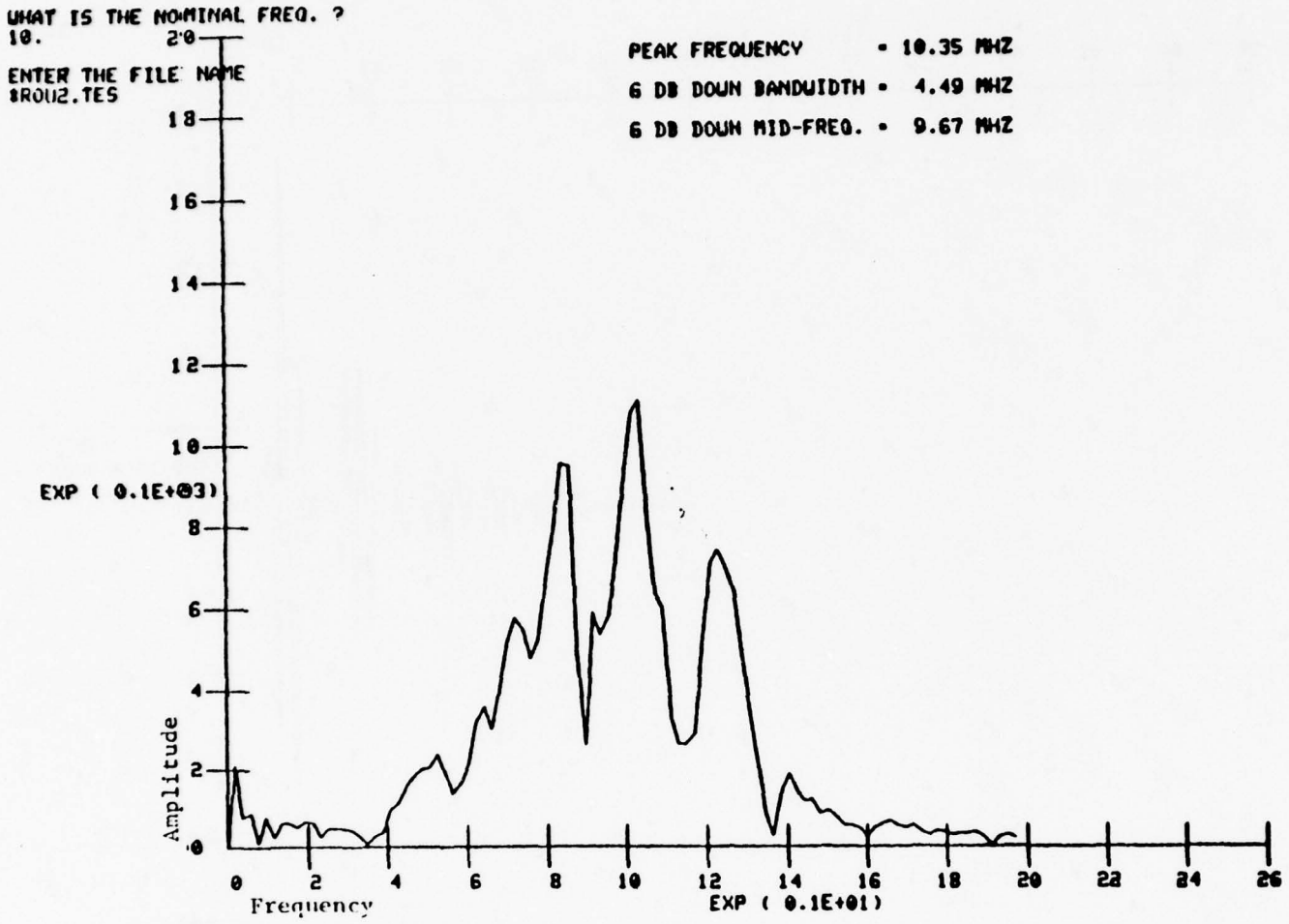

Figure 15B. Signal Spectrum

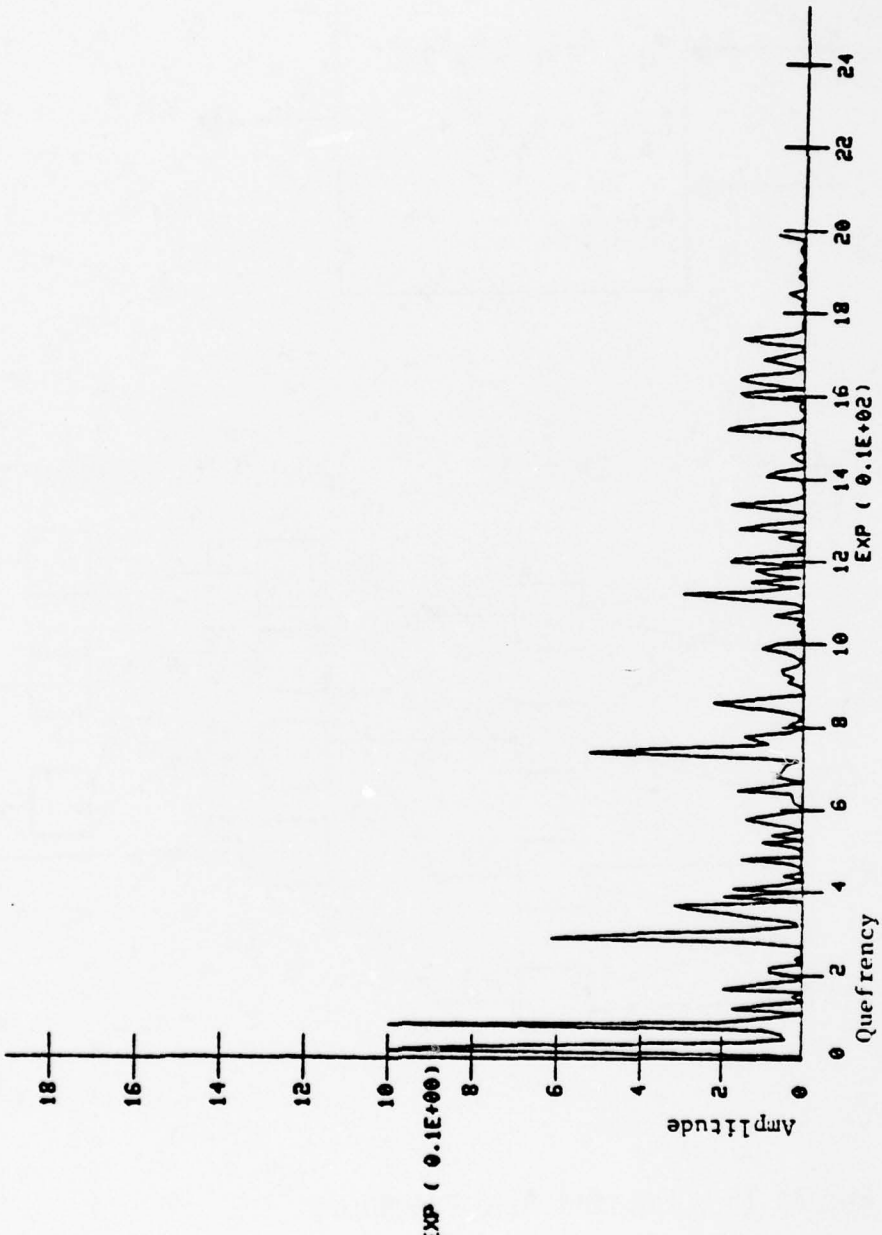

Figure 15C. Signal Cepstrum

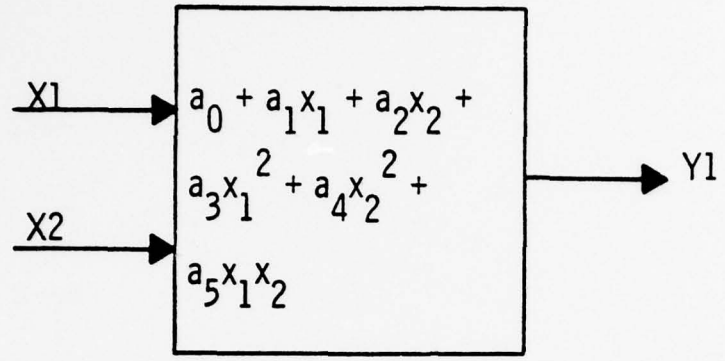

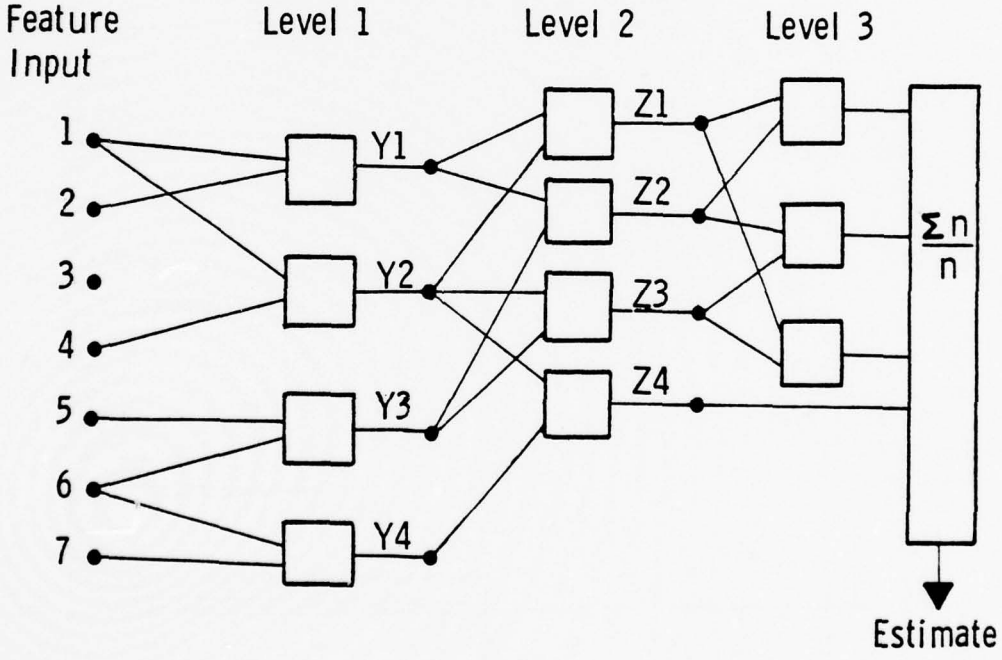

Figure 16. Example ALN Procedure

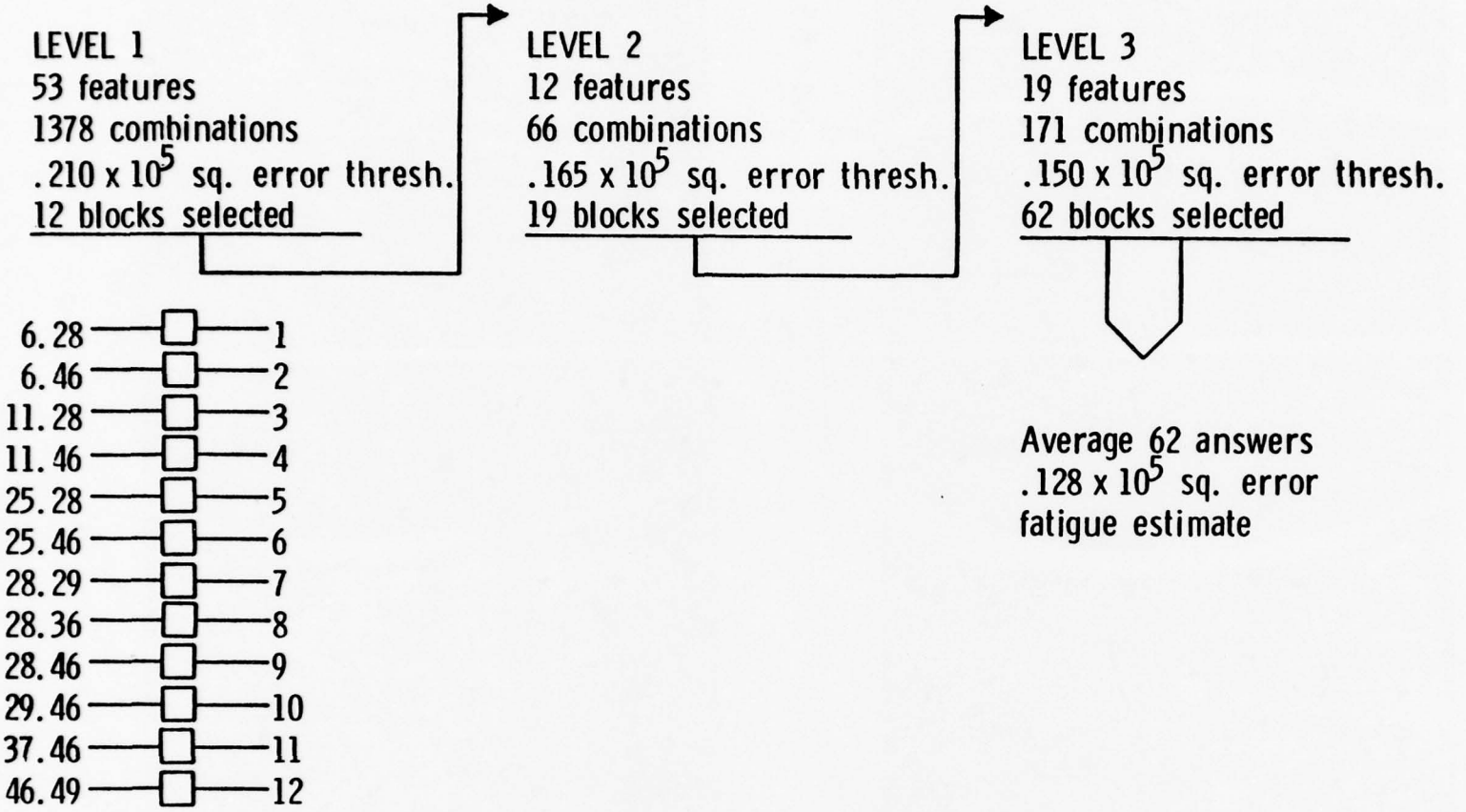

Figure 17. Outline of Solution ALN

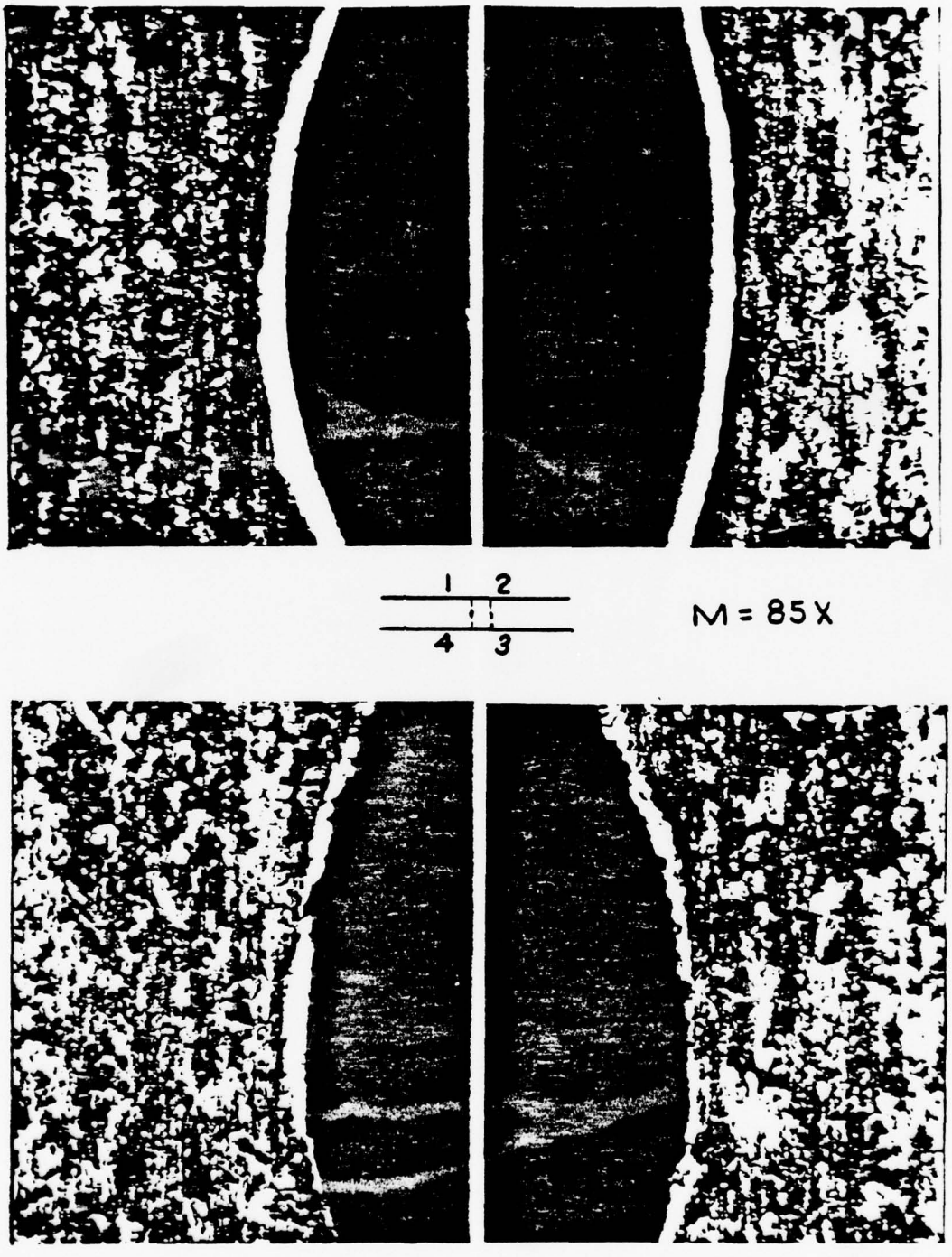

Figure 18A. Surface Cracks at 10% Fatigue Life

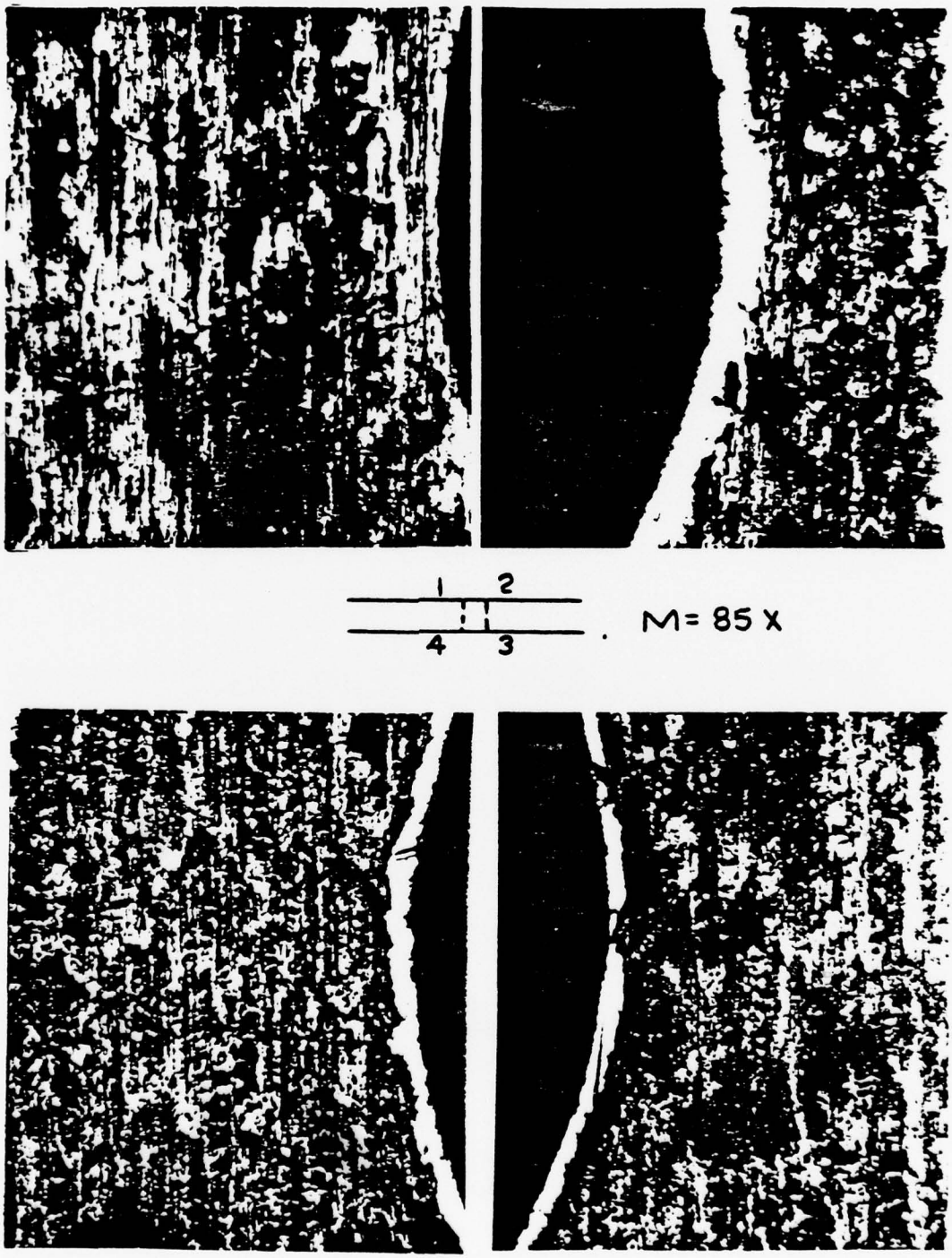

Figure 18B. Surface Cracks at 20% Fatigue Life

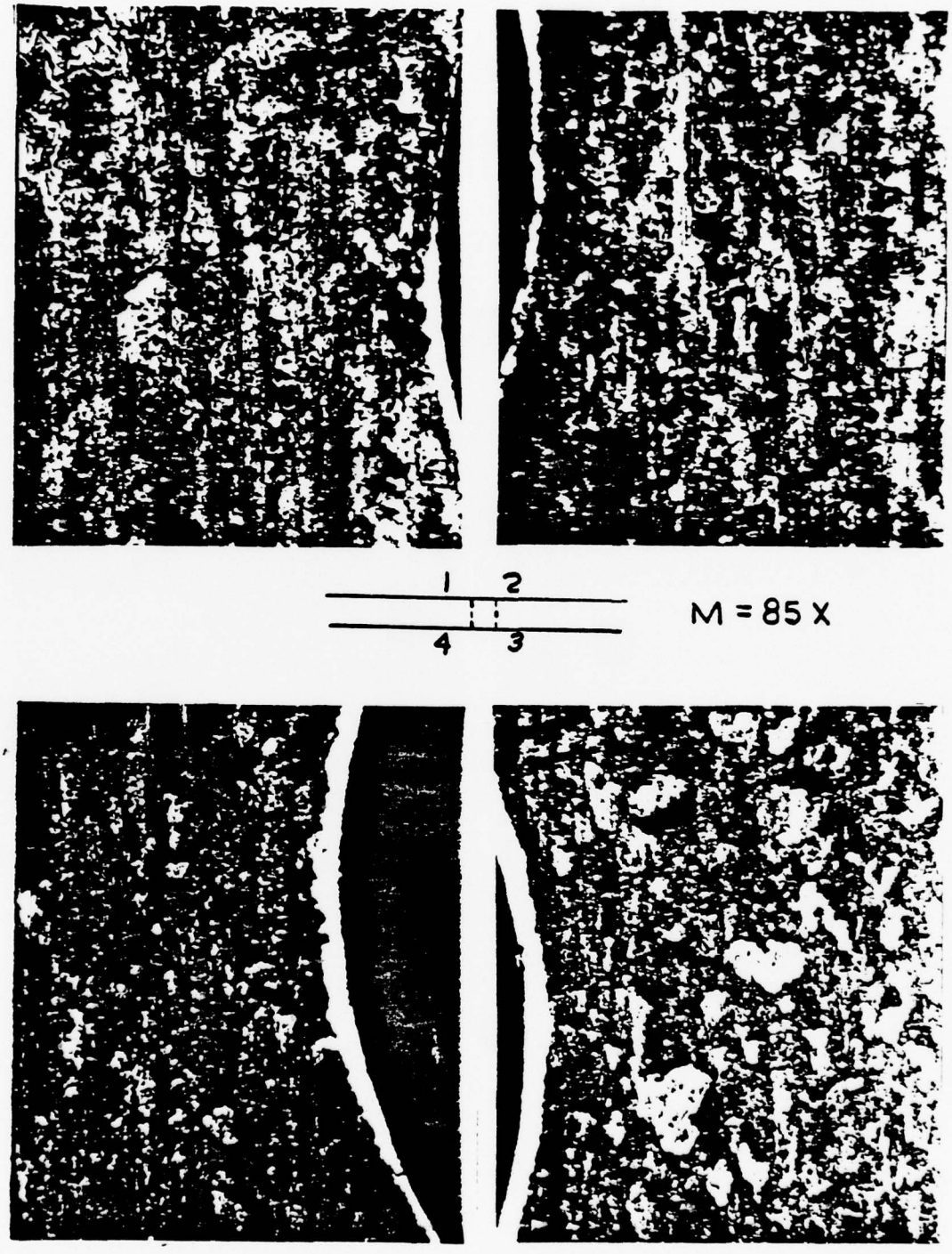

Figure 18C. Surface Cracks at 30% Fatigue Life

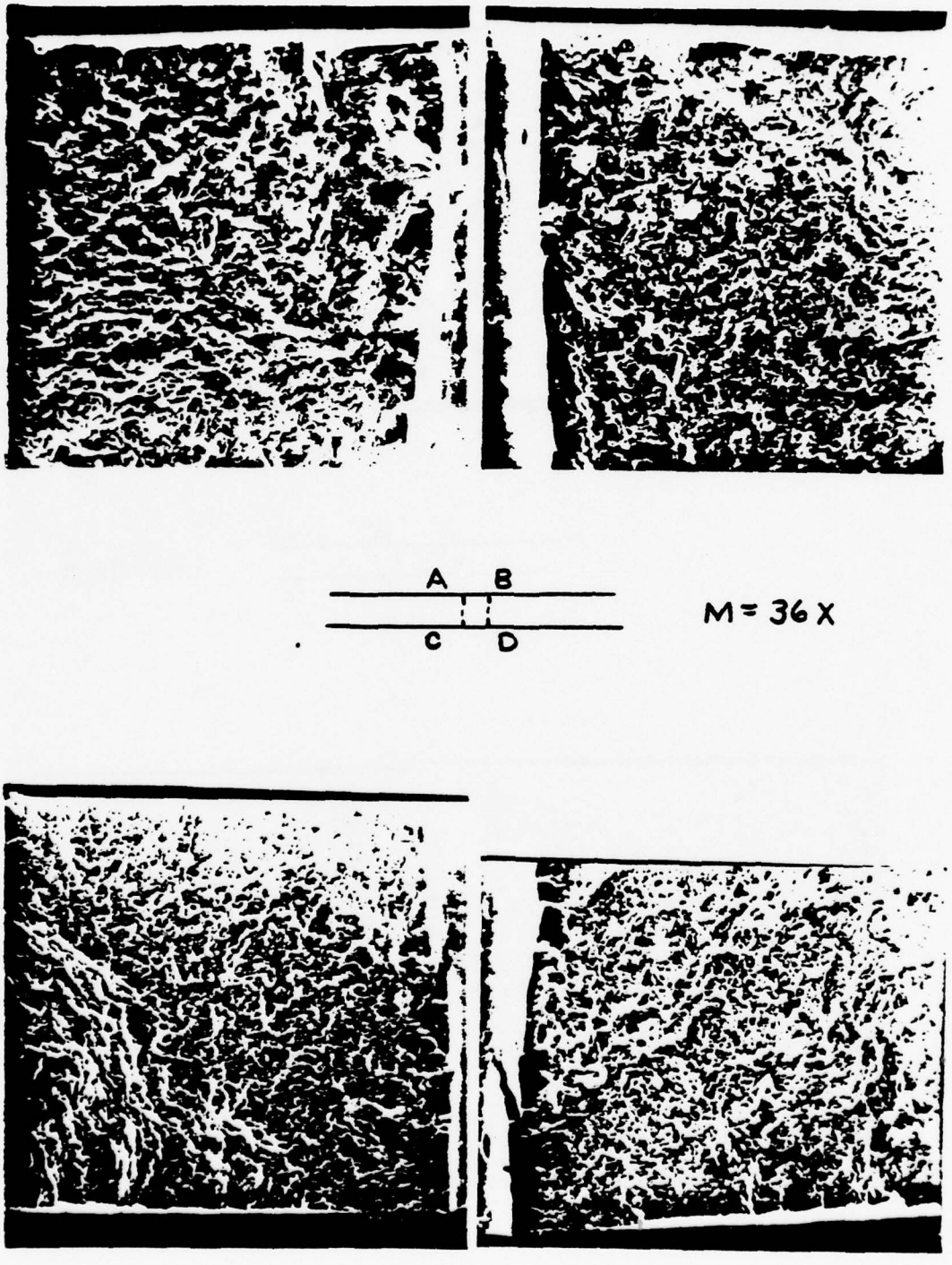

Figure 19A. Fracture Surface at 10% Fatigue Life

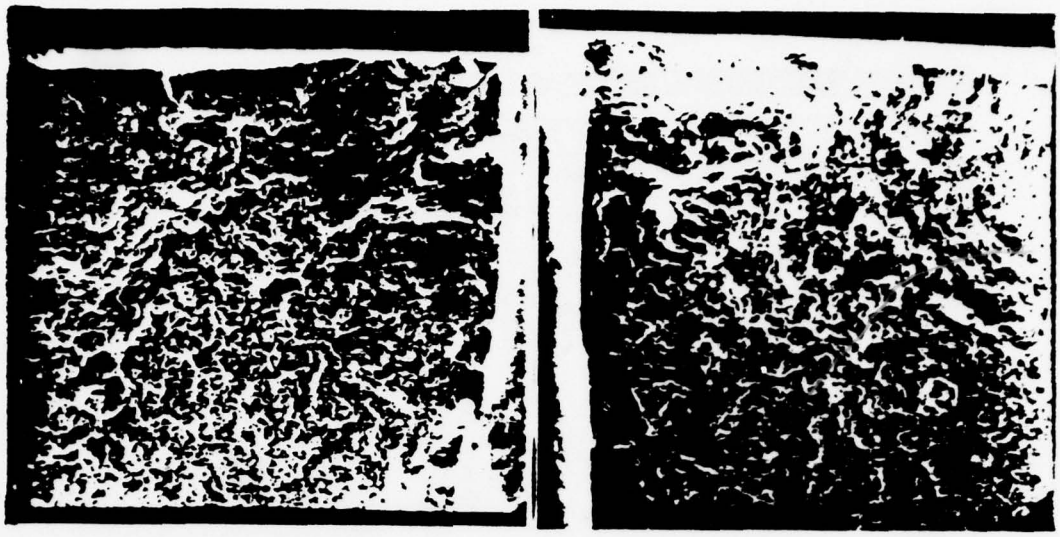

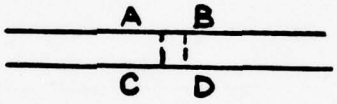

M=36 X

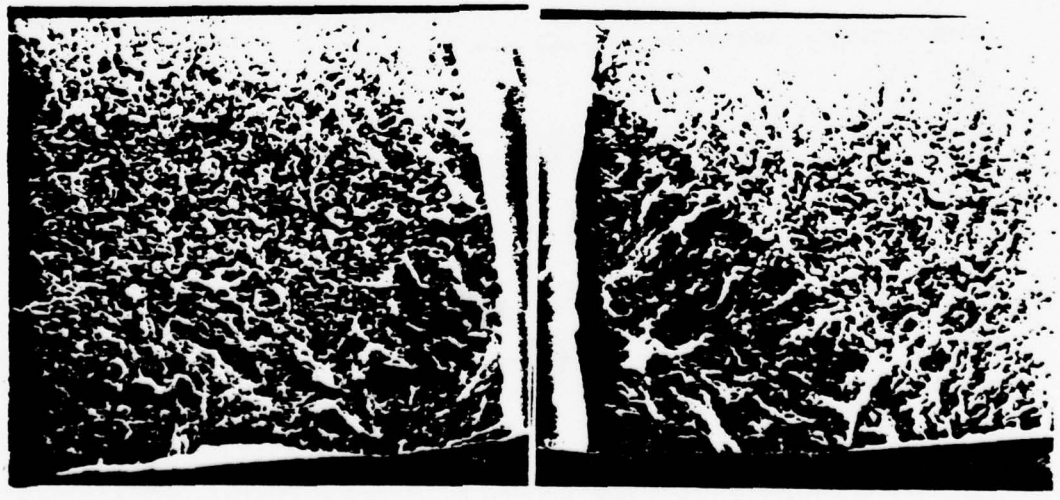

Figure 19B. Fracture Surface at 20% Fatigue Life

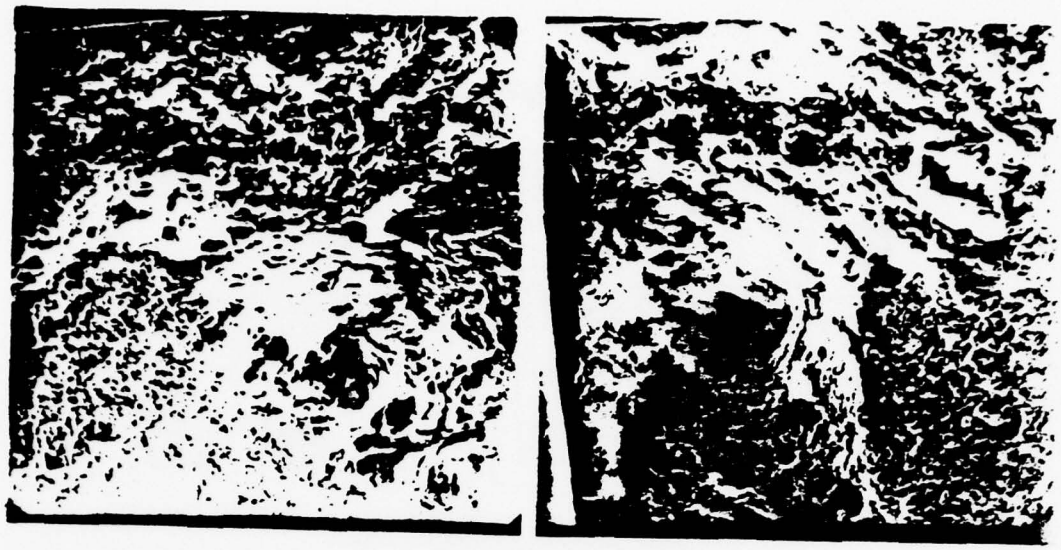

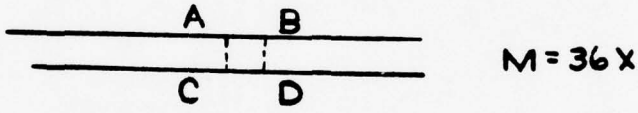

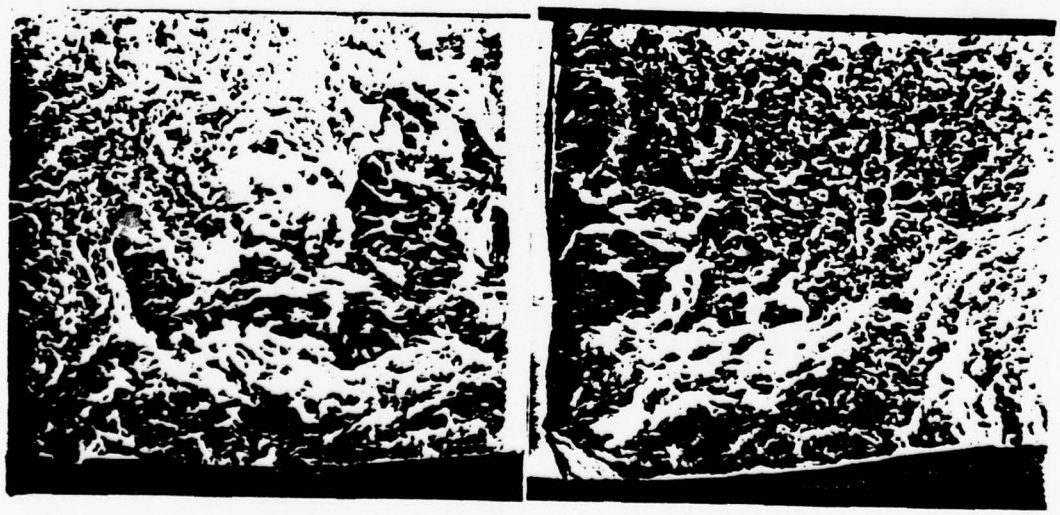

Figure 19C. Fracture Surface at 30% Fatigue Life

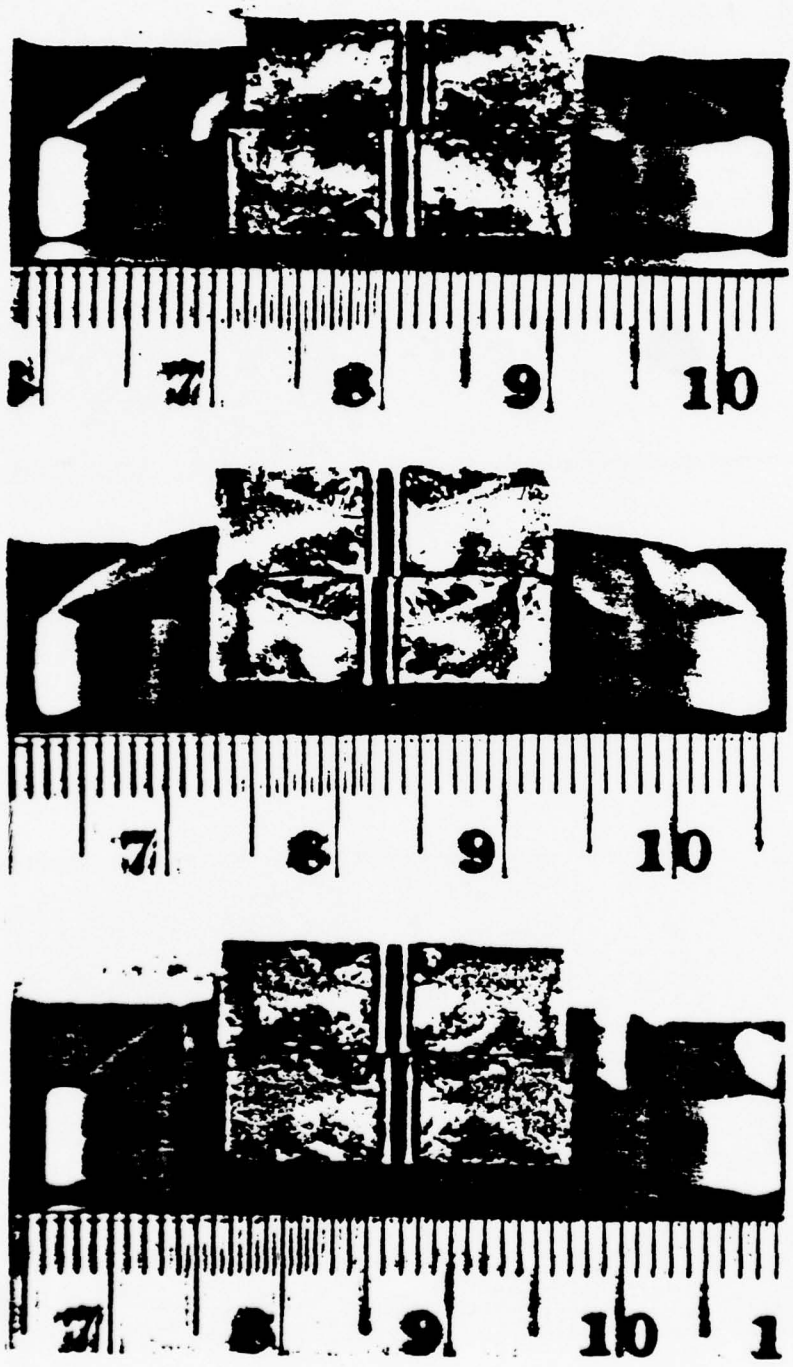

Figure 20. Typical Fatigue Fracture Surfaces

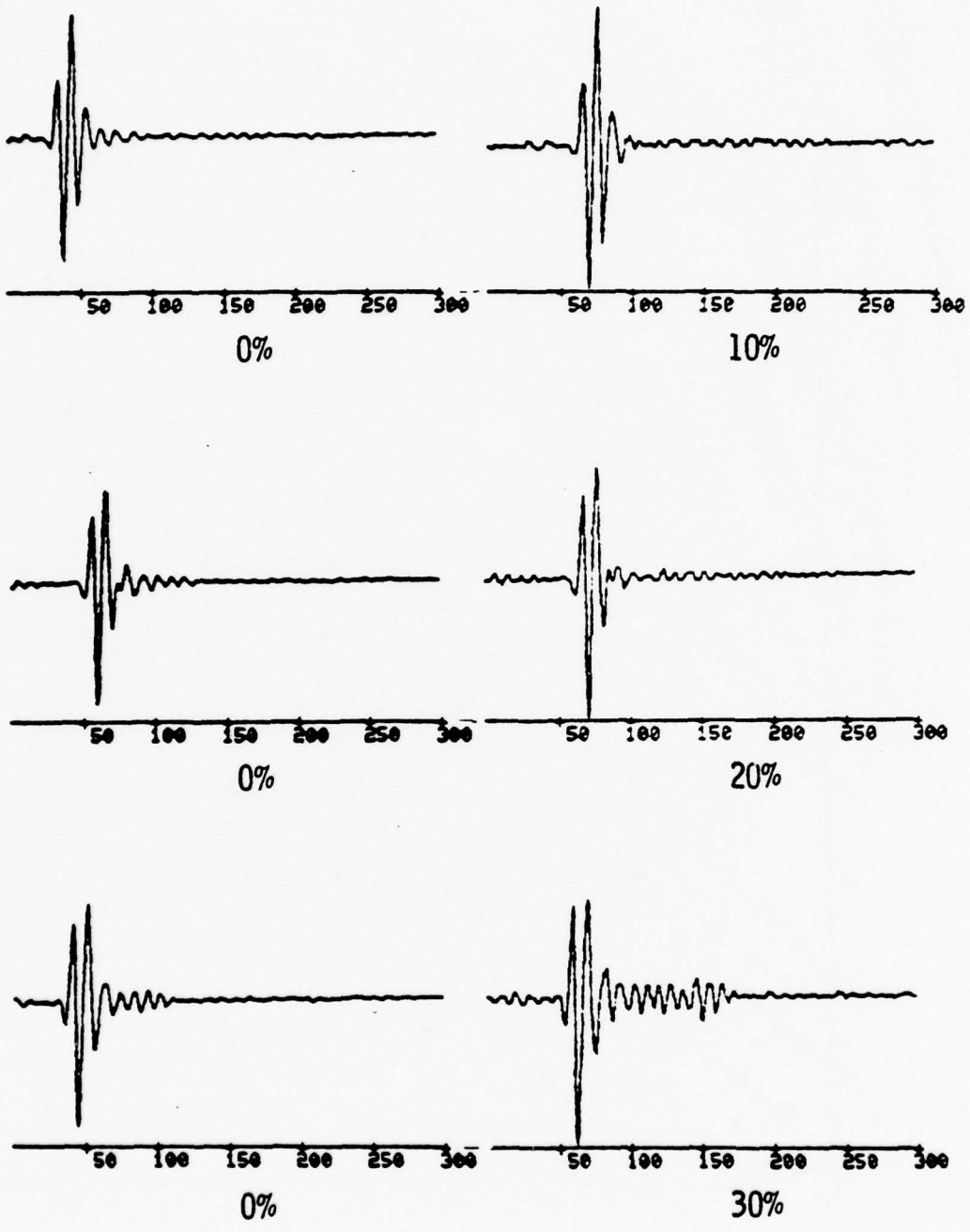

Figure 21. Amplitude Time Signals for 10%. 20%. and 30% Fatigue Life Specimens

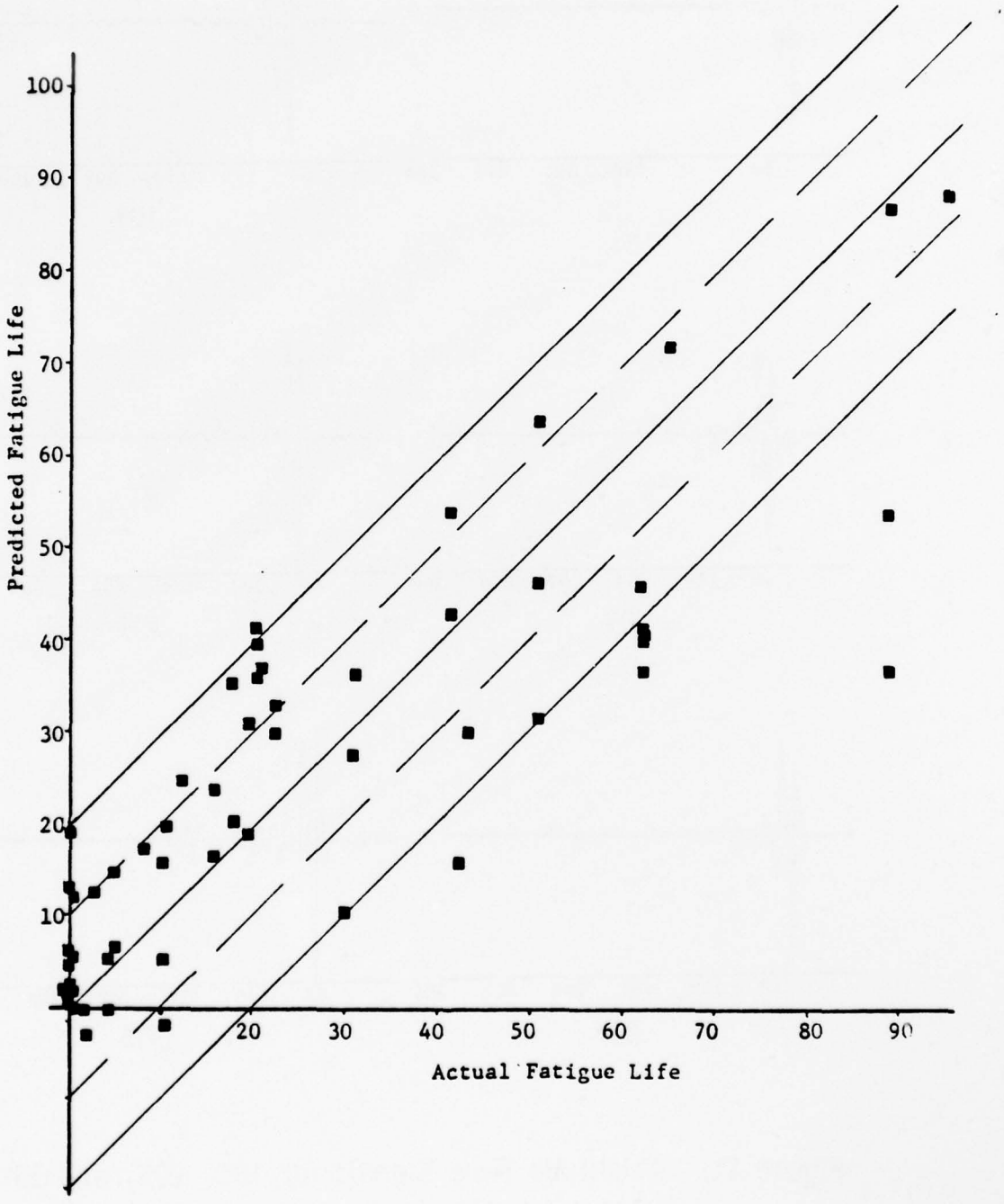

Figure 22. Training Data: Actual vs. Predicted Fatigue Life

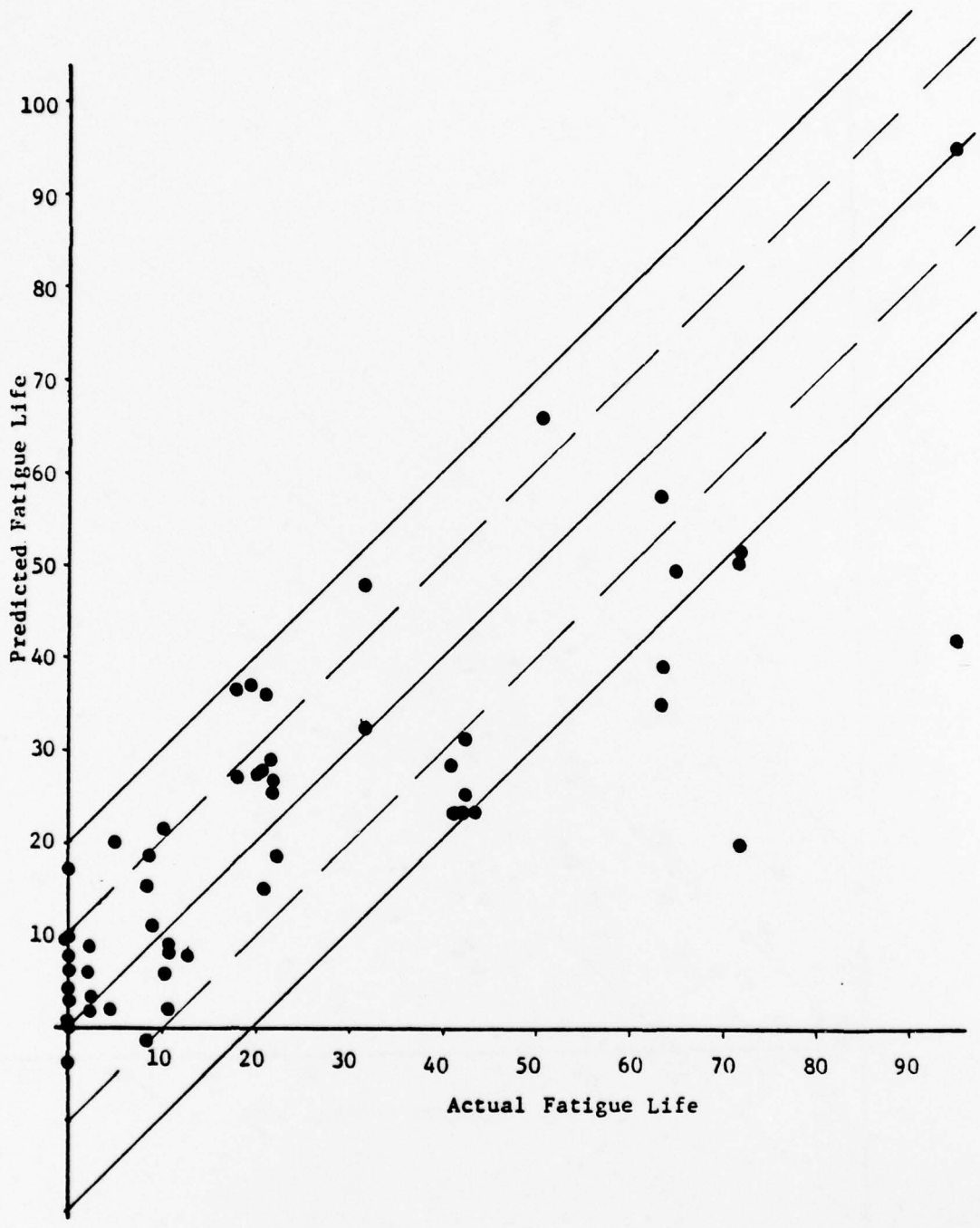

Figure 23. Selection Data: Actual vs. Predicted Fatigue Life

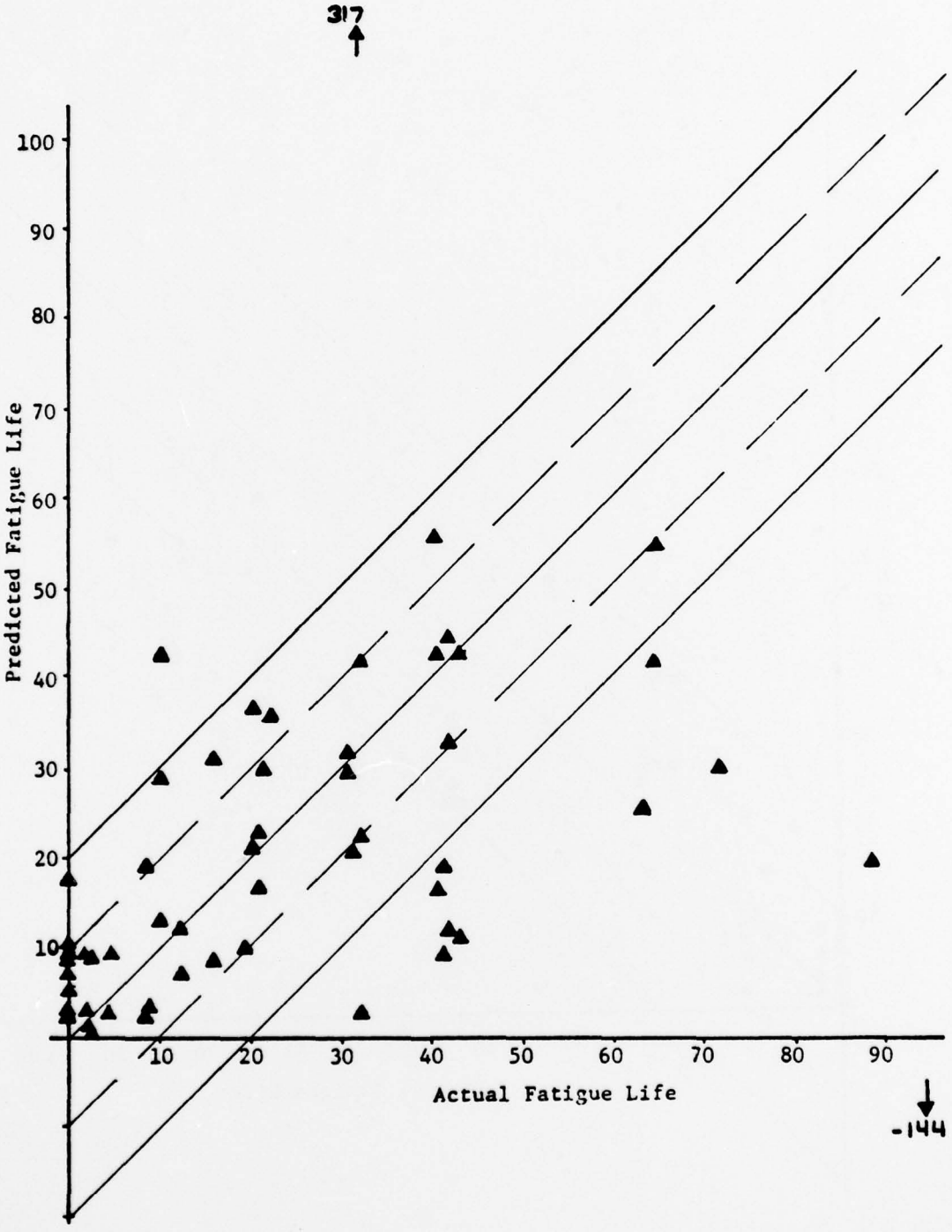

Figure 24. Test Data: Actual vs. Predicted Fatigue Life

APPENDICES

APPENDIX A

TRANSDUCER CHARACTERISTICS

A computer automated transducer characterization procedure has been developed by Mr. M. Good of Drexel University. The tests consist of axial pressure profiles, beam symmetry measurements, and transducer frequency measurements from signal reflections from rod and plate targets at various distances from the transducer. A water couplant is used. The records for the Aerotech transducer used in this study appear on the following pages.

NORMAL BEAM TRANSDUCER PERFORMANCE SPECIFICATION MEASUREMENT CHART

1. MISCELLANEOUS

A. TRANSDUCER DIAMETER "D" ---------0.63 CM
B. SPECIFIED FREQUENCY "F" -------10.00 MHZ
C. BROAD OR NARROW BAND ---------BROAD BAND
D. CRYSTAL TYPE ----------
E. SERIAL NUMBER AND/OR CODE ----------
F. TEST EQUIPMENT USED IN THE EVALUATION
---

2. CENTER FREQUENCY MEASUREMENT CF

A. WATER PATH LENGTH D ----------NEAR FIELD
B. TARGET MATERIAL -SS BOUND ROD, GROUND E
C. ACTUAL CENTER FREQUENCY CF ----8.22 MHZ
D. CENTER FREQUENCY ERROR, (F - CF)/F X 100 = ----18.25 PERCENT
E. CENTER FREQUENCY TOLERANCE = ----------5.0 PERCENT
F. ACCEPTABE (YES OR NO) ----------NO

3. FREQUENCY CLASSIFICATION
(BROAD BAND CLASSIFICATION BRANCH)

A. CENTER FREQUENCY CF ------8.22 MHZ B. A = ------1.56 MHZ C. B = ------1.95 MHZ D. U = -----3.51 MHZ
E. CALCULATED BANDWIDTH TOLERANCE ----4.39 MHZ (GREATER THAN 50% OF CF) F. BWF = U - 1A-B1 ---3.12 MHZ G. ACCEPTABLE BWF -------YES (YES OR NO)
H. CALCULATED OFFSET TOLERANCE -------0.62 MHZ AT 6DB (20% OF BWF) I. ACTUAL OFFSET AT --0.39 MHZ 6DB 1A-B1 J. ACCEPTABLE OFFSET ----YES (YES OR NO)

4. SPURIOUS FREQUENCY CONTENT

A. CF ----------8.22 MHZ B. CFA ----------6.24
C. QIMAX ----------0.24 D. QIMAX TOLERANCE ----------0.62 (LESS THAN 10% OF CFA) E. ACCEPTABLE QIMAX ----------YES (YES OR NO)

*MUSE --

Table A1. Transducer Performance Chart

5. RESOLUTION CAPABILITY
(BROAD BAND CLASSIFICATION BRANCH)

A. CALCULATED RC' TOLERANCE ___0.296E=01_CM (LESS THAN 2 LAMBDA)
B. RC ___0.284E=01_CM
C. ACCEPTABLE RC _____NO (YES OR NO)

6. NEAR FIELD EVALUATION

A. TARGET DISCRIPTION
(1) MATERIAL _____STAINLESS_STEEL
(2) TYPE _____ROUND_ROD,_GROUND_FINISH
(3) SIZE _____.64_CM_OUTER_DIAMETER
(4) DISTANCE _____

B. NEAR FIELD CALCULATIONS, N _____6.81_CM
C. ACTUAL NEAR FIELD MEASUREMENT N' _____6._CM
D. PERCENT ERROR = (N'-N) / N __=11.91_PERCENT
E. TOLERANCE _____5.0_PERCENT
F. ACCEPTABLE N' (YES OR NO) _____NO

7. PRESSURE OSCILATION WITHIN THE NEAR FIELD
(BROAD BAND CLASSIFICATION BRANCH)

A. TARGET DISCRIPTION
(1) MATERIAL _____STAINLESS_STEEL
(2) TYPE _____ROUND_ROD,_GROUND_FINISH
(3) SIZE _____.64_CM_OUTER_DIAMETER
(4) DISTANCE _____

B. CALCULATED ALLOWABLE _____LESS_THAN_6_DB DB VARIATION
C. ACTUAL DB VARIATION, DB' _____1.94_DB
D. ACCEPTABLE DB VARIATION _____YES (YES OR NO)

8. BEAM SYMMETRY MEASUREMENT

A. TARGET DISCRIPTION
(1) MATERIAL _____STAINLESS_STEEL
(2) TYPE _____ROUND_ROD,_GROUND_FINISH
(3) SIZE _____.64_CM_OUTER_DIAMETER
(4) DISTANCE _____

>MUSE --

Table A1 (cont.). Transducer Performance Chart

```
B.  FIRST MEASUREMENT, PRESSURE VERSUS X

    (1) A' ----------0.85_CM    (2) B' ----------0.88_CM    (3) BUP ----------0.33_CM

    (4) OFFSET AT 6DB ------0.17_CM    (5) OFFSET TOLERANCE ------0.02_CM    (6) ACCEPTABLE OFFSET ----------NO
        |A'-B'|                        AT 6DB ( 5.% OF BUP)                      (YES OR NO)

C.  SECOND MEASUREMENT, PRESSURE VERSUS Y

    (1) A' ----------0.88_CM    (2) B' ----------0.13_CM    (3) BUP ----------0.81_CM

    (4) OFFSET AT 6DB ------0.85_CM    (5) OFFSET TOLERANCE ------0.01_CM    (6) ACCEPTABLE OFFSET ----------NO
        |A'-B'|                        AT 6DB ( 5.% OF BUP)                      (YES OR NO)
STOP --
```

Table A1 (cont.). Transducer Performance Chart

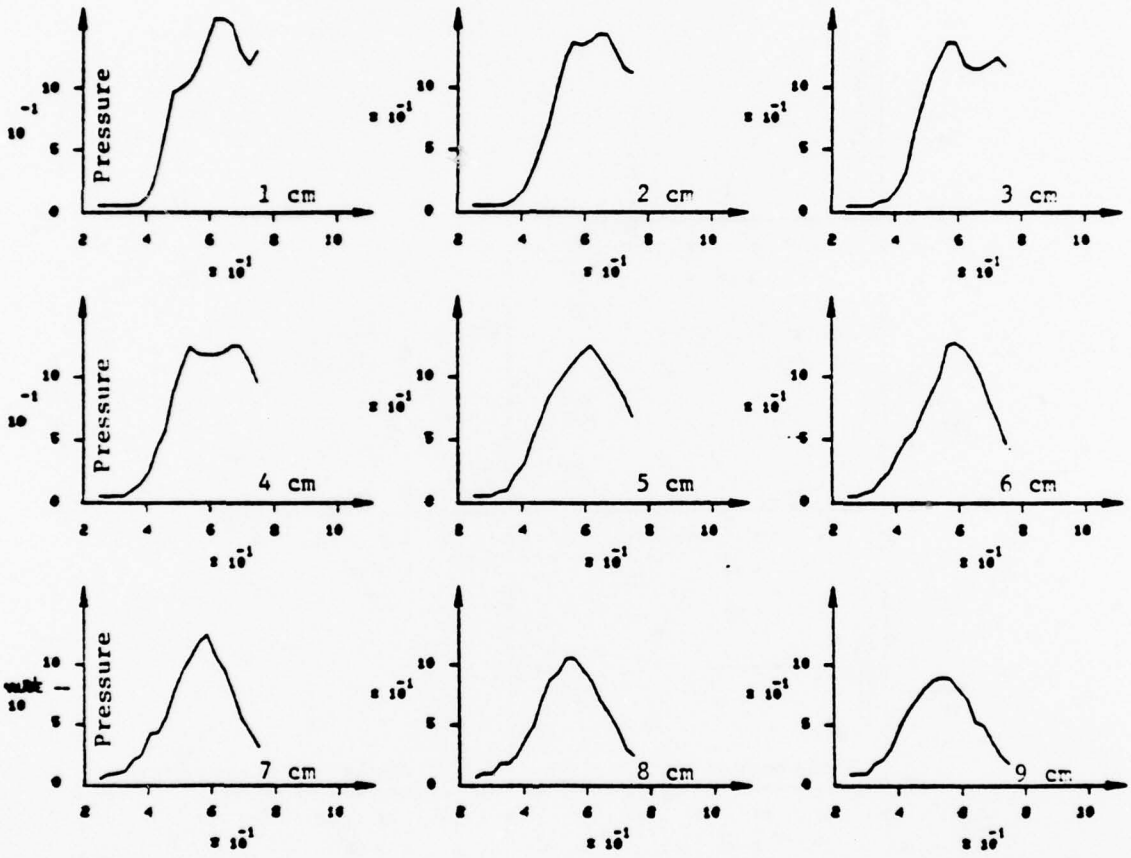

Figure A1. Axial Pressure Profiles at 1-10 cm

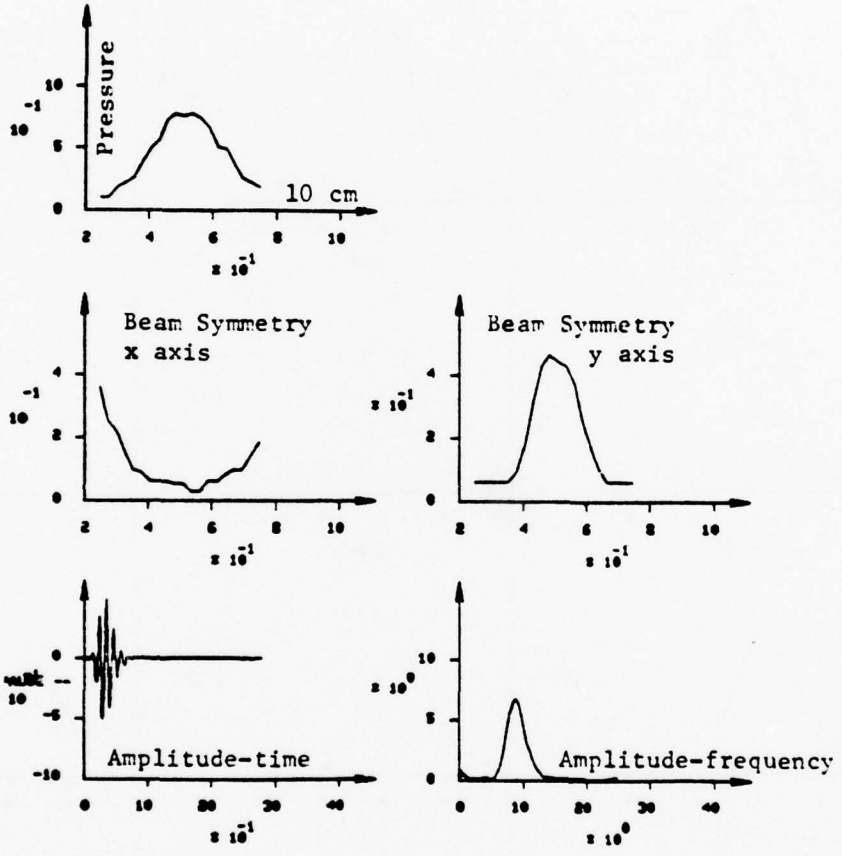

Figure A2. Transducer Beam Symmetry and Frequency Characteristics

APPENDIX B

TEST CODE

Each specimen is interrogated by transducers in eight locations. A complete test requires two transducer locations, thus each specimen produces four tests (Figure 7). The data from a single transducer location was stored under a code name consisting of five digits and two letters. A breakdown of the Code is illustraded below:

01	-	specimen number
6	-	transducer location (1-8)
15	-	estimated percent fatigue life used.
.		
GG	-	aerotech gamma transducer with pulser set to standard test conditions

Note from Figure 7 that every two transducer locations form a test pair and that even numbers are close to the hole and interrogate the plate bottom surface while odd number locations are distant from the hole and examine the top plate surface.

APPENDIX C

FRACTURE MECHANICS SOLUTION OUTLINE

Since this work attempts to measure fatigue damage rather than the more conventional crack length, it is useful to relate the number of cycles to failure (N_f) to the initial crack size (ai) that can be sensed. A procedure by which this can be done, assuming the functional relationships for stress intensity (K) and crack growth rate (da/dN) are known, is outlined below.

1. Know the stress intensity relation for the particular part and crack geometry. In general stress intensity is a function of nominal stress (σ), crack length (a) and some geometry correction factor (Q).

$$K = \sigma Q (\pi a)^{\frac{1}{2}} \qquad (C1)$$

2. Know the critical stress intensity (Kc or KIc) for the material involved. Using equation (C1), the critical flaw size (a_f), the flaw size that would produce failure at stress , can be calculated.

3. Measure or estimate an initial flaw size (ai). This has often been set at the minimum size detectable.

4. A subcritical flaw can grow to a critical size due to fatigue loading. Determine the rate of crack growth for the material. A simple form is

$$da/dN = A \Delta K^n \qquad (C2)$$

where A and n are experimental material values and K is the stress intensity range for cyclic loading.

5. Combine equations (C1 and (C2), separate the N and a terms, and integrate between zero and N_f cycles and cracks lengths ai and a_f to obtain an expression for remaining life.

$$\frac{da}{dN} = A(1.77\Delta\sigma Q)^n a^{n/2} \tag{C3}$$

$$\int_{a_i}^{a_f} \frac{da}{a^{n/2}} = A(1.77\Delta\sigma Q)^n \int_0^{N_f} dN \quad \text{for } n \neq 2 \tag{C4}$$

$$N_f = \frac{2}{(n-2)A(1.77\Delta\sigma Q)^n}\left(\frac{1}{a_i^{(n-2)/2}} - \frac{1}{a_f^{(n-2)/2}}\right) \tag{C5}$$

Since a_f is usually much larger than ai it can be ignored. Thus, the number of cycles to failure is directly related to the initial flaw size that can be detected.

UNCLASSIFIED

SECURITY CLASSIFICATION OF THIS PAGE *(When Data Entered)*

REPORT DOCUMENTATION PAGE		READ INSTRUCTIONS BEFORE COMPLETING FORM
1. REPORT NUMBER N00014-77-C-0607	2. GOVT ACCESSION NO.	3. RECIPIENT'S CATALOG NUMBER
4. TITLE *(and Subtitle)* An Ultrasonic Nondestructive Test Procedure for the Early Detection of Fatigue Damage and the Prediction of Remaining Life.		5. TYPE OF REPORT & PERIOD COVERED First Annual Report, no. 1-3
		6. PERFORMING ORG. REPORT NUMBER
7. AUTHOR(s) James M. Carson Joseph L. Rose		8. CONTRACT OR GRANT NUMBER(s) N00014-77-C-0607 mcw
9. PERFORMING ORGANIZATION NAME AND ADDRESS Drexel University 32nd & Chestnut Sts. Phila., PA 19104		10. PROGRAM ELEMENT, PROJECT, TASK AREA & WORK UNIT NUMBERS NR 064-583
11. CONTROLLING OFFICE NAME AND ADDRESS Department of Navy, Office of Naval Research Structural Mechanics Program Arlington, VA 22217		12. REPORT DATE August 1978 13. NUMBER OF PAGES 90
14. MONITORING AGENCY NAME & ADDRESS *(if different from Controlling Office)* 12 23p.		15. SECURITY CLASS. *(of this report)* 15a. DECLASSIFICATION/DOWNGRADING SCHEDULE

16. DISTRIBUTION STATEMENT *(of this Report)*

Approved for Public Release; Distribution Unlimited

17. DISTRIBUTION STATEMENT *(of the abstract entered in Block 20, if different from Report)*

18. SUPPLEMENTARY NOTES

19. KEY WORDS *(Continue on reverse side if necessary and identify by block number)*

Fatigue	Ultrasonics
Remaining Life	Crack
Nondestructive Testing	Cepstrum

20. ABSTRACT *(Continue on reverse side if necessary and identify by block number)*

The goal of nondestructive testing may be simply expressed as the detection and complete specification (size, shape, orientation, etc.) of flaws. This is seldom possible, however. The most dangerous flaw is one that is crack-like or that serves as a crack initiation site. A procedure to detect and estimate fatigue damage occurring at such a site is reported.

A computer based data acquisition system is used to analyze data

DD FORM 1 JAN 73 1473 EDITION OF 1 NOV 65 IS OBSOLETE

S/N 0102-LF-014-6601

UNCLASSIFIED

SECURITY CLASSIFICATION OF THIS PAGE *(When Data Entered)*

390 782

CONT

from 2024-T4 Al fatigue specimens containing a through hole. Specimens are fatigue loaded to produce a spectrum of damage levels and interrofated using a simple contact 10 MHz shear wave system. Features selected from the signal amplitude time, spectrum, and cepstrum signatures are used in a computer learning network to make an early detection of fatigue damage and a quantitative prediction of remaining life. A scanning microscope is used to examine the damage at the limit of detection.

Fatigue damage was sensed with 92% success after 10% of specimen life. Estimates of damage were made within ± 20 of the actual fatigue life percentage for 76% of the data.

+ OR −